ELUCIDATING THE ROLE OF YEAST LIPIN (*PAH1*) IN LIPID DROPLET BIOGENESIS

APPROVED BY SUPERVISORY COMMITTEE

_____
Joel M. Goodman

_____
Michael G. Roth

_____
Katherine J. Luby-Phelps

_____
Philipp E. Scherer

ACKNOWLEDGEMENTS

I am grateful to many people here at The University of Texas Southwestern Medical Center at Dallas and other institutions for their encouragement and assistance throughout the course of this research. In Particular, I'd like to thank Dr. Kent Chapman and Patrick Horn at The University of North Texas for their mass spectrometric analysis of *pah1Δ* mutants. Members of the pharmacology department Dr. Melanie Cobb and Dr. Paul Sternweis as well as the members of my committee, Dr Michael Roth, Dr. Katherine Luby-Phelps and Dr. Philipp Scherer for their encouragement and guidance during the course of this research.

Special Thanks to the current members of the Goodman Lab, without whom, this work would not have been possible. And finally, Dr. Joel Goodman for his unwavering support and enthusiasm towards the work done and his excellent guidance, caring, and patience during my stay in his lab. Thank you so much.

ELUCIDATING THE ROLE OF YEAST LIPIN (*PAH1*) IN LIPID DROPLET BIOGENESIS

by

OLUDOTUN ADEYO

DISSERTATION

Presented to the Faculty of the Graduate School of Biomedical Sciences

The University of Texas Southwestern Medical Center at Dallas

In Partial Fulfillment of the Requirements

For the Degree of

DOCTOR OF PHILOSOPHY

The University of Texas Southwestern Medical Center at Dallas

Dallas, Texas

September, 2011

ELUCIDATING THE ROLE OF YEAST LIPIN (*PAH1*) IN LIPID DROPLET BIOGENESIS

Oludotun Adeyo, Ph.D.

The University of Texas Southwestern Medical Center at Dallas, 2011

Supervising Professor: Joel M. Goodman, Ph.D.

Lipid droplets are unique organelles important for a host of cellular functions including the storage of neutral lipids, but factors that regulate the biogenesis and maintenance of these organelles remain relatively unknown. The primary focus of this dissertation will be to understand the role of the phosphatidic acid hydrolase (Pah1p) in the biogenesis of lipid droplets in *Saccharomyces cerevisiae*. Pah1p is an enzyme that converts phosphatidic acid to diacylglycerol, and its absence or elimination of its catalytic activity results in the accumulation of neutral lipids within membranes of the endoplasmic reticulum. Furthermore, lipid droplet formation is facilitated by diacylglycerol through a mechanism that appears to be independent of diacylglycrol's role as a substrate for triglyceride biosynthesis. Finally, lipid droplets originated from regions of the endoplasmic reticulum where the Pah1p activators were located.

The second part of this dissertation will focus on the lipodystrophy related protein Fld1p and its association with lipid droplets. Droplets always associate with Fld1p, and in the absence of lipid droplets, Fld1p is localized as patches distributed throughout the endoplasmic reticulum. In addition, induced lipid droplets originate from these Fld1 patches.

I conclude from this work that diacylglycerol facilitates lipid droplet formation and that Fld1p is somehow involved in the biogenesis or maintenance of these organelles.

TABLE OF CONTENTS

PUBLICATIONS

O. Adeyo, P. J. Horn, S. Lee, D. Binns, A. Chandrahas, K. D. Chapman, J. M. Goodman. The Yeast Lipin Ortholog Pah1p is Important for Biogenesis of Lipid Droplets. *The Journal of Cell Biology*. 192: 1043-1055.

ABSTRACTS

O. Adeyo, S. Lee, A. S. Chandrahas, J. M. Goodman. Diacylglycerol Generated by Lipin Acts in Packaging of Neutral Lipids into Cytoplasmic Droplets. *The 49th annual meeting of the American Society for Cell Biology*, San Diego, CA, USA, December 5 – 9, 2009. #104/B51

S. Han, **O. Adeyo**, D. Binns, N. Grishin, J. Goodman. A Human *SPO7* Candidate That Forms a Phosphatase Complex with Dullard to Activate Lipin. *The 50th annual meeting of the American Society for Cell Biology*, Philadelphia, PA, USA, December 11 – 15, 2010. #2110/ B431

FIGURES

TABLES

LIST OF ABBREVIATIONS

ATP	Adenosine Triphosphate
NADH	Nicotinamide Adenine Dinucleotide
TAG	Triglycerides/ Triacylglycerol
StE	Steryl Esters
PC	Phosphotidylcholine
PE	Phosphotidylethanolamine
PI	Phosphotidylinositol
PS	Phosphotidylserine
ADRP	Adipose Differentiation Related Protein
TIP-47	Tail Interacting Protein of 47 kDa
PKA	Protein kinase A
HSL	Hormone Sensitive Lipase
ATGL	Adipose Triglyceride Lipase
ER	Endoplasmic Reticulum
CGI-58	Comparative Gene Identification-58
HCV	Hepatitis C Virus
DGAT	Diglyceride Acyltransferase
PA	Phosphatidic Acid
DAG	Diacylglycerol
PAP	Phosphatidic Acid Phosphatase
N-LIP	Amino-terminal Lipin Domain
C-LIP	Carboxy-terminal Lipin Domain

mTORC1	Mechanistic Target Of Rapamycin Complex 1
SREBP	Sterol Regulatory Element-Binding Protein
BODIPY	4-bora-3a, 4a-diaza-s-indacene
OD	Optical Density
SD	Synthetic Dextrose media
PNS	Post-Nuclear Supernatant
TLC	Thin Layer Chromatography
EM	Electron Microscopy
SCD	Synthetic Complete Dextrose media
LD	Lipid Droplets

CHAPTER 1

GENERAL INTRODUCTION

Living organisms require energy for all aspects of life. Cells fulfill this requirement by generating energy-rich molecules such as ATP and NADH through a series of oxidation reactions on ingested or absorbed nutrients. When energy is abundant, it is stored in cellular reservoirs in the form of polysaccharides and lipids. In animal cells, polysaccharides such as glycogen are stored in cytoplasmic glycogen granules and serve as a secondary means of energy storage primarily in liver and muscle tissue. Glycogen in muscle tissues can be readily converted to glucose satisfying short-term energy needs. On the other hand, glucose as well as other absorbed nutrients can be converted into lipids, and stored within adipose tissues in the form of triglycerides (TAG) and steryl esters (StE) in unique intracellular organelles called lipid droplets.

Very little is known about the biogenesis of lipid droplets and how they contribute to disease. Enlargement of lipid droplets and proliferation of adipose tissue is central to the obesity epidemic (Faust et al., 1978). On the other hand, the ability of a cell to make lipid droplets prevents free fatty acids from being driven towards non-oxidative pathways that form reactive lipids that promote lipotoxicity and eventually lipoapoptosis of cells. Furthermore, ectopic accumulation of lipids in liver and skeletal muscle tissues has severe impacts on

overall body metabolism. Therefore, understanding the biogenesis of lipid droplets could provide insights into their nature and role in disease.

The goal of this dissertation was to understand what role the *Saccharomyces cerevisiae* lipin orthologue (*PAH1*) plays in lipid droplet biogenesis.

Biology of a Lipid Droplet

Lipid droplets were once considered as relatively benign lipid storage compartments within cells. However, in recent years they are now being recognized as dynamic organelles important for a host of cellular functions, including functions not related to lipid metabolism.

Lipid Droplet Structure

Conversion of fatty acids and sterols into neutral lipids that are subsequently stored in lipid droplets is a storage strategy that has been conserved from prokaryotes to eukaryotes (Murphy, 2001; Waltermann and Steinbuchel, 2005). Lipid droplets vary greatly in size with diameters ranging from 1 – 5 μm in nonadipocytes, but can be greater than 100 μm in white adipocytes (Fujimoto and Parton, 2011). The current paradigm of lipid droplet structure suggests that lipid droplets are made up of a lipid ester core, and unlike other organelles they are

surrounded by only a monolayer of phospholipid and numerous proteins; some of which are important for lipid droplet biology.

The core of a lipid droplet is made up of lipid esters predominantly TAG and/ or StE coexisting in various ratios. However, the possibility exists that some free cholesterol and phospholipids may also reside within the core (Hevonoja et al., 2000). It has been proposed that in some circumstances, the lipid esters within the core may segregate from each other, partitioning themselves into regions of StE, TAG and fatty acid compositional variants of TAG (Cheng et al., 2009; Czabany et al., 2008). This suggestion is made due to evidence obtained from cryo-electron microscopy studies that show concentric lipid ester layers (presumably sterol esters) within the lipid droplet core (Tauchi-Sato et al., 2002), as well as onion skin like fracture faces observed by freeze fracture electron microscopy(Baba et al., 1995; Tauchi-Sato et al., 2002).

Phospholipids are the predominant compounds at the monolayer of the lipid droplet and are generally similar to those in the endoplasmic reticulum. They include phosphotidylcholine (PC), phosphotidylethanolamine (PE), phosphotidylinositol, lysoPC and lysoPE (Bartz et al., 2007; Leber et al., 1994; Tauchi-Sato et al., 2002). However, free cholesterol may also reside within the droplet monolayer (Prattes et al., 2000).

Proteins on the lipid droplet surface may be adherent to the phospholipid monolayer or embedded in it by extending long helical hairpins through the

monolayer into the core (Capuano et al., 2007). Although it is energetically unfavorable, some studies have also shown the presence of proteins within the lipid droplet core (Bozza et al., 1997; Dvorak et al., 1992; Robenek et al., 2005; Robenek et al., 2004). It has been suggested that amphiphilic proteins may bind to phospholipids making a complex that is compatible with the hydrophobic environment of the lipid droplet core (Fujimoto and Parton, 2011).

Proteomic analysis has revealed lipid droplet associated proteins involved in lipid metabolism and transport, intracellular trafficking, signaling, chaperone function, RNA metabolism and cytoskeletal organization (Bartz et al., 2007; Beller et al., 2006; Brasaemle et al., 2004; Liu et al., 2004; Sato et al., 2006; Wan et al., 2007). The composition of these proteins on the lipid droplet surface varies between lipid droplets within a cell, by metabolic conditions, and cell type. Some of the most studied lipid droplet-associated proteins are the members of the PAT-domain (Perilipin, ADRP and TIP-47) family which regulate the interface between lipid droplets and their cellular environment. For example, β-adrenergic receptor activation by catecholamines initiate signaling cascades that result in protein kinase A (PKA) phosphorylation of perilipin, a member of the PAT-domain family that prevents access of lipases to stored triglycerides. Phosphorylation of perilipin triggers lipolysis by allowing the cytosolic hormone sensitive lipase (HSL) to dock on lipid droplets, and activation of the lipid

droplet- associated adipose triglyceride lipase (ATGL) (Miyoshi et al., 2007; Wang et al., 2009).

Lipid Droplet Biogenesis:

Light and electron microscopic evidence from a variety of cell types indicate that lipid droplets are often associated or connected with the ER. Furthermore, enzymes that synthesize the neutral lipids present in the droplet core localize predominantly on the ER, suggesting that the observed ER lipid droplet interactions occur to facilitate the transfer of newly synthesized neutral lipids into lipid droplets (Robenek et al., 2006). These evidence as well as the observation that multiple ER proteins (such as calnexin and immunoglobulin heavy chain binding protein (BiP)) are found in lipid droplet fractions has led to the suggestion that they originate from the ER (Brasaemle et al., 2004; Liu et al., 2004; Umlauf et al., 2004).

Several hypotheses on how lipid droplets can originate from the ER have been proposed, but none have been sufficiently proven or refuted by current experimental data. The most cited model suggests that droplets originate from the synthesis of neutral lipids between the bilayer of the ER. Deposited neutral lipids eventually grow outward toward the cytoplasm as a bud that may or may not detach from the ER, but nevertheless forms the structure defined as a lipid droplet.

Another model suggests that specialized domains on the ER exist for lipid droplet formation using the vesicle formation machinery of the secretory pathway. Lipid droplets start off as small bilayer vesicles (Walther and Farese, 2009). While associated with the ER, neutral lipids are synthesized between the membrane bilayer of the nascent vesicle such that the vesicular lumen makes up only a small portion of the lipid droplet structure. The lumen may either fuse with the outer membrane of the droplet or remain as an inclusion within the droplet. A role for coatamer proteins in droplet formation is supported by the fact that knockdown or inhibition of the COPI/ Arf1 vesicular transport machinery interferes with lipid droplet formation (Guo et al., 2008; Nakamura et al., 2005).

The third model is one that suggests that the lipid droplet is excised from the ER with the droplet monolayer containing both lumenal and cytoplasmic leaflets of the ER. Although the excision model would result in the creation of a transient hole in the ER membrane, it does explain the presence of transmembrane ER proteins on the surface of lipid droplets (Ploegh, 2007).

Lipid Droplet Functions:

Over the years lipid droplets have been linked with several cellular functions that are largely regulated by proteins associated with the droplet. The major function ascribed to lipid droplets is the storage of lipid esters; a process regulated in part by members of the PAT-domain family of proteins.

Overexpression of ADRP increases the storage of neutral lipids in droplets by preventing lipolysis through the action of adipose triglyceride lipase (ATGL) (Listenberger et al., 2007). ADRP overexpression also decreases microsomal neutral lipid content while its deletion enhances storage of neutral lipids in microsomes, suggesting that ADRP plays a role in promoting the formation of lipid droplets from the ER (Chang et al., 2006). Proteins other than members of the PAT-family such as fat-inducing proteins 1 and 2 (FIT1 and FIT2) have also been shown to be important for the formation of lipid droplets albeit without increasing triglyceride synthesis or decreasing lipolysis (Kadereit et al., 2008).

Neutral lipids aren't just stored in lipid droplets for later use; they also function to buffer cells from the toxic effects of excessive amounts of lipids. Storage of free fatty acids in the form of triacylglycerol protects against fatty acid induced lipotoxicity, and storage of cholesterol as cholesterol esters prevents ER stress and eventual cell death that would occur in the absence of such a buffering mechanism. For example, yeast cells not able to synthesize neutral lipids survive under normal laboratory growth conditions, but undergo membrane proliferation and cell death when supplemented with unsaturated fatty acids (Petschnigg et al., 2009).

Neutral lipids stored in lipid droplets can also be utilized when needed to provide lipids required for assembling components of biological membranes or the generation of energy. This function is initiated by the action of protein lipases

that reside on (or are targeted to) the lipid droplet surface. In *Saccharomyces cerevisiae* deletion of the ATGL orthologue Tgl4p results in membrane deficiency and a delayed entry into the cell cycle (Kurat et al., 2009). Other metabolites from lipolysis such as diacylglycerol and monoacylglycerol may also have signaling roles within the cell.

Enzymes involved in fatty acid activation and steroid synthesis have also been observed in isolated lipid droplet fractions (Goodman, 2009). It is assumed that a certain percentage of these proteins are microsomal contaminants present in the droplet isolates, because some of the observed proteins span membrane bilayers and are not likely to reside in the monolayer of the lipid droplet. The excision model for droplet biogenesis attempts to incorporate this finding. Furthermore, there is differing activity for some of these enzymes depending on the cellular fraction with which the assay was performed, suggesting a physiological relevance to the dual localization of these proteins (Fujimoto and Parton, 2011; Goodman, 2009).

Lipid Droplets and Disease

Misregulation of lipid droplet functions or ectopic formation of droplets in cells that otherwise would not have them are hallmarks of some metabolic diseases. Lipid droplets would obviously play a role in diseases such as obesity that are a result of excess triacylglycerol storage and often lead to the

development of type 2 diabetes and cardiovascular problems. In conjunction with their role in regulating access of lipases to lipid droplets, perilipin-null and transgenic mice have been shown to be resistant to diet induced obesity (Miyoshi et al., 2010; Qi et al., 2004). Loss-of-function mutations in genes encoding lipid droplet proteins involved in the regulation of lipolysis (such as CGI-58 and ATGL) also cause neutral lipid storage diseases as well as icthyosis and myopathy (Fischer et al., 2007; Schweiger et al., 2009).

Lipodystrophies are a group of disorders characterized by the loss of adipose tissue, fatty liver, hypertriglyceridemia and insulin resistance. The cause of this disorder has been linked to mutations in genes for lipid droplet-associated proteins such as seipin and caveolin-1 (Kim et al., 2008; Magre et al., 2001; Szymanski et al., 2007).

Gain-of-toxic-function mutations to seipin as well as mutations to the TIP-47 binding protein (Spartin) have been linked to motor neuron diseases such as silver syndrome and Troyer syndrome (Eastman et al., 2009; Patel et al., 2002; Windpassinger et al., 2004).

Finally, unconventional roles for lipid droplets in the propagation of infectious agents within cells have been observed. Lipid droplets are important for the later stages of the hepatitis C virus (HCV) lifecycle. The HCV replication complex localizes close to lipid droplets, its viral core protein targets to lipid droplets in a diglyceride acyltransferase 1 (DGAT1) dependent manner, and the

lipoprotein synthesis pathway is required for the assembly of the lipoviroparticle (Herker et al., 2010; McLauchlan, 2009; Miyanari et al., 2007; Syed et al., 2010). Dengue virus also exploits lipid droplets for particle formation (Samsa et al., 2009). Finally, the intracellular pathogen *Chlamydia trichomatis* utilizes lipids derived from its host for its growth (Kumar et al., 2006).

Lipin

Triacylglycerol stored in the lipid droplet core is synthesized through sequential acylation of glycerol-3-phosphate resulting in phosphatidic acid. The subsequent dephosphorylation of phosphatidic acid (PA) to make diacylglycerol (DAG) is the penultimate step before triacylglycerol synthesis can occur, and is also required for the synthesis of membrane phospholipids phosphotidylcholine and phosphotidylethanolamine. The dephosphorylation of PA is an essential step for the synthesis of phospholipids and neutral lipids in mammalian cells, and it links the two halves of the phosphoglycerolipid synthesis pathways; i.e. the synthesis of PI, PS and PE from PA via the CDP-DAG pathway and the synthesis of PC from DAG in the final steps of the Kennedy pathway. Lipins are a family of magnesium-dependent phosphatidic acid phosphatase enzymes that catalyze the dephosphorylation of PA to DAG (Han et al., 2006). They are proteins of about 100 KDa in size that contain a conserved amino-terminal (N-LIP) domain, and a

carboxy-terminal catalytic domain (C-LIP) containing a DXDXT motif. In mammals, the C-LIP domain also has a nuclear localization signal.

Unlike all other enzymatic reactions involved in the synthesis of TAG, a majority of PAP activity was observed to be in soluble fractions of cell lysates (Hubscher et al., 1967), but found to translocate to membrane fractions possibly regulated by phosphorylation or fatty acids (Brindley, 1984). Since lipins lack transmembrane domains, they must translocate from the cytosol to membranes to perform their function. This translocation appears to be regulated by protein kinases.

Lipin in Mammals:

The first lipin gene (*Lpin1*) was originally identified by positional cloning from a spontaneously-mutated mouse that showed decreases in adipose tissue mass, transient fatty liver and peripheral neuropathy; symptoms similar to lipodystrophy (Klingenspor et al., 1999; Langner et al., 1989; Peterfy et al., 2001; Rehnmark et al., 1998; Reue et al., 2000). The lipin family in mammals consists of three genes (lipin 1, lipin 2 and lipin 3), which exhibit different tissue expression patterns and variable PAP activity (V_{max} lipin 1 >> lipin 2 > lipin 3) (Donkor et al., 2007). The main feature linking the lipin paralogues is the high conservation of their N-LIP and C-LIP domains, the latter of which contains the catalytic site required for PAP activity (Peterfy et al., 2001).

Mammalian lipin is regulated by phosphorylation which controls its activity by altering its cellular localization. Hyperphosphorylation of lipin results in its association with 14-3-3 proteins and its cytosolic retention (Harris et al., 2007; Peterfy et al., 2010). Dephosphorylation by protein phosphatases directs lipin to ER compartments or into the nucleus in adipocytes and hepatocytes. At the ER, the lipin substrate (phosphatidic acid) is available for conversion to diacylglycerol. DGAT at the ER then acylates diacylglycerol to generate the triacylglycerides stored within the core of a lipid droplet. In the nucleus, mammalian lipin (specifically lipin 1) acts as a transcriptional co-activator of fatty acid oxidation and adipogenic genes (Finck et al., 2006; Koh et al., 2008). It was reported recently that the mechanistic target of rapamycin complex 1 (mTORC1), a nutrient and growth factor-responsive kinase, regulates the localization of lipin 1to control the sterol regulatory element binding protein (SREBP) pathway (Peterson et al., 2011).

Lipin in Yeast:

Yeast, as well as most other invertebrates expresses a single lipin ortholog. In *Saccharomyces cerevisiae* this is Pah1p, the first PAP enzyme to be characterized at a molecular level (Han et al., 2006). Confirming its role as a PAP enzyme, a knockout of *PAH1* results in decreases in DAG and TAG levels, a concomitant increase in PA and several changes in phospholipid levels (Han et

al., 2006). Although Pah1p lacks the nuclear localization signal observed in mammalian lipin, chromatin immunoprecipitation studies have shown that a pool of Pah1p-protein A-fusion protein may interact with promoters of genes involved in phospholipid biosynthesis (Santos-Rosa et al., 2005).

Regulation of Pah1p Function:

Similar to mammalian lipins, Pah1p is also known to be regulated by phosphorylation. In yeast, Pah1p is dephosphorylated by a transmembrane protein phosphatase complex consisting of Nem1p and Spo7p (Santos-Rosa et al., 2005; Siniossoglou et al., 1998). Nem1p is the catalytic subunit of the complex and a member of the CPD protein phosphatase family, while Spo7p is the regulatory subunit required for Nem1p phosphatase activity and binds to its catalytic domain (Kobor et al., 1999; Santos-Rosa et al., 2005). Dephosphorylation of Pah1p by the Nem1p-Spo7p phosphatase complex enhances Pah1p activity and allows it to interact with the ER membrane via a short amino-terminal amphipathic helix (Karanasios et al., 2010). This interaction permits the production of DAG for TAG and phospholipid biosynthesis at the membrane.

Pah1p is phosphorylated at many sites by multiple protein kinases which results in cytoplasmic retention of Pah1p and decreases its PAP activity. Candidate Pah1p kinases include cell cycle kinases such as Cdc28p, Pho85p and the Dbf2p-Mob1p complex (Dephoure et al., 2005; Mah et al., 2005; Ptacek et al.,

2005; Santos-Rosa et al., 2005). Seven of the multiple phosphorylation sites on Pah1p contain Ser/Thr-Pro (S/T-P) motifs, some of which are known to be targeted by the Nem1p-Spo7p phosphatase complex (O'Hara et al., 2006). This is consistent with data showing that yeast *NEM1* and *SPO7* deletion mutants have hyperphosphorylated Pah1p and display relatively similar structural phenotypes as *pah1Δ* (Santos-Rosa et al., 2005; Siniossoglou et al., 1998). A summary of the Pah1p pathway describing its involvement in neutral lipid synthesis is diagrammed in Figure 1.

Regulation of Phospholipid Biosynthesis by Pah1p:

As mentioned earlier, Pah1p lacks a nuclear localization signal but it can regulate genes encoding enzymes involved in phospholipid biosynthesis by regulating phosphatidic acid levels. In *Saccharomyces cerevisiae* the level of PA controls the transcription of genes that encode enzymes involved in the CDP-DAG and Kennedy pathways (Carman and Henry, 2007). PA performs this role by regulating the localization of Opi1p, a PA binding protein and transcriptional repressor (Loewen et al., 2004; White et al., 1991). Low PA levels at the ER membrane would release Opi1p, allowing it to translocate to the nucleus to repress UAS_{INO} regulated genes (phospholipid biosynthetic genes contain UAS_{INO} promoters (Loewen et al., 2004)). The converse would occur (derepression of UAS_{INO} and therefore increased synthesis of its regulated genes) when PA levels

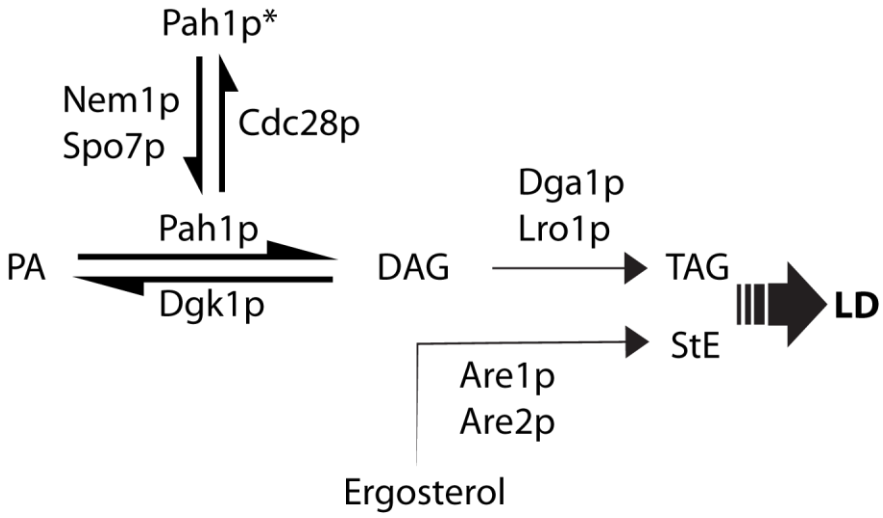

Figure 1. Simplified diagram outlining the final steps in neutral lipid synthesis. Pah1p*, phosphorylated cytosolic Pah1p; LD, lipid droplet; TAG, triacylglycerol; StE, steryl ester.

are high, as occurs in *pah1Δ* cells, in which the increase in PA and subsequently PI and PE results in nuclear/ ER membrane proliferation (Santos-Rosa et al., 2005).

Project History and Dissertation Aim

The laboratory of Dr. Joel Goodman attempts to understand organelle biogenesis and maintenance, and in recent years the organelle in focus has been the lipid droplet. To understand factors that regulate lipid droplet biogenesis and maintenance, a haploid *Saccharomyces cerevisiae* deletion library of non-essential genes was screened for mutants with abnormal lipid droplet morphology (Szymanski et al., 2007). The screen was performed by staining cells, cultured in rich media to both logarithmic and stationary phases of growth, with a neutral lipid dye 4-bora-3a, 4a-diaza-s-indacene 493/ 503 (BODIPY) to visualize lipid droplets by fluorescence microscopy. From 4,936 deletion strains, 59 were observed to have abnormal lipid droplet morphology, and included deletion mutants of the membrane protein phosphatases discussed earlier: Nem1p and Spo7p. In these mutants, BODIPY stained lipid droplets as well as ring like structures assumed at the time to be the endoplasmic reticulum (Szymanski et al., 2007). A similar phenotype was later observed for yeasts strains that lacked the substrate for the phosphatase complex, Pah1p (Adeyo et al., 2011).

The unifying theme for all the lipid biogenesis models is that the organelle originates from the ER. Considering this, I hypothesized that the BODIPY-stained ER ring phenotype, observed for *NEM1*, *SPO7* and *PAH1* mutants was due to a defect in the biogenesis of lipid droplets, with the assumption that some of the neutral lipids are trapped in the ER and unable to form droplets. The primary focus of this dissertation will be to test this hypothesis, and to understand the role Pah1p plays in the biogenesis of lipid droplets.

CHAPTER 2

Pah1p IS IMPORTANT FOR LIPID DROPLET FORMATION

Introduction

Previous work in the Goodman lab demonstrated that the neutral lipid dye (BODIPY) stained lipid droplets as well as membranous structures (assumed at the time to be the endoplasmic reticulum) in cells that lack *PAH1* or its protein phosphatases Nem1p and Spo7p (Szymanski et al., 2007). Concurrent with the proposed models for lipid droplet biogenesis, I hypothesized that membrane staining represented neutral lipids trapped within the ER indicative of a role played by Pah1p in the transfer of neutral lipids from the ER into droplets during droplet biogenesis.

In this chapter, the presence of neutral lipids in the ER of *pah1Δ* mutants will be confirmed and subcellular distribution of neutral lipid classes will be investigated. I will also demonstrate that the defect in lipid droplet formation observed in the absence of *PAH1* is not a result of an expected decrease in triglyceride synthesis.

Materials and Methods

Strains and Culture Conditions

All yeast strains and plasmids used in this chapter are listed in Table 1.

Except for growth in oleic acid containing medium, all yeast strains used in this study were cultured at 30 ºC in minimal medium containing 2.0 % glucose, 0.67 % Yeast Nitrogen Base (Difco Labs, Detroit, MI) and the appropriate amino acid supplements to prevent the loss of plasmids. Except for growth in oleic acid containing media, data for all experiments were obtained from cells in exponential phase growth (OD_{600} of 0.4 – 0.6) For oleic acid grown cultures, cells grown in minimal liquid medium were diluted to 0.10 OD_{600}/ mL in minimal SD media containing 0.20 % glucose for 30 hours. 1.0 OD_{600} was then transferred to oleic acid medium which contained: 0.5 % potassium phosphate buffer pH 6.0, 0.3 % yeast extract, 0.5 % peptone, 0.1 % (v/v) oleate and 0.2 % (v/v) Tween-80.

DNA Manipulations

All plasmids used in this study are listed in Table 1. Standard recombinant DNA techniques were used. Bacterial strain DH10β (Invitrogen) was used for all bacterial transformations. *PAH1* knockout in OAS001, OAS002 and OAS003 strains was performed by homologous recombination using a DNA cassette containing ~500 bp of *PAH1* sequence (from the 5' and 3' untranslated region

flanking *PAH1* ORF) ligated to opposite ends of a *TRP1* sequence. Yeast strains were transformed by the lithium acetate method (Ito et al., 1983). DNA manipulations resulting in changes to coding sequence as well as changes to genome were verified by sequence performed by the McDermott Center for Human Growth and Development (University of Texas Southwestern Medical Center, Dallas, TX).

Fluorescence Microscopy

For the acquisition of static images, strains were stained with BODIPY 493/503 (Invitrogen) (Szymanski et al., 2007) to visualize lipid droplets and transformed (where listed) with pRS315-PGK-CFP-HDEL to visualize the ER. Cells in log phase were removed from growth medium, concentrated by centrifugation (3,000 x g for 5 min at room temperature), and suspended on microscope slides in growth medium containing 1% agar (Kron, 2002). All images were acquired using Slidebook software (version 4.1.0.3, Intelligent Imaging Innovations) on a microscope (Axiovert 200M; CarlZeiss Microimaging, Inc) with a 100x 1.3 NA oil immersion objective lens (plan-Neofluar) equipped with a digital camera (Sensicam; Cooke). BODIPY images were acquired using the fluorescein isothiocyanate filter set, CFP with the CFP filter set and Nile Red and Oil Red O with the CY3 filter set (Chroma Technology Corp.). Z-stacks were obtained at 0.3-μm spacing, and Slidebook commands of deconvolution (nearest

neighbor option) were used to build three dimensional image stacks through cells. For Figure 3 the range of pixel intensities used for the control strain to clearly visualize droplets were fixed and used for the other strains in the series so the images can be directly compared. When droplets were to be counted, cells were fixed using the fixation method required for Nile Red staining.

To visualize Nile Red-stained cells, samples were fixed in 2% (v/v) formaldehyde and incubated for 1 minute at room temprature, washed twice in Tris pH 7.5 buffer before observation (Wolinski and Kohlwein, 2008). For Oil Red O-stained cells, samples were washed with H_2O and resuspended in freshly filtered Oil Red O solution (3 parts of 1% stock in isopropanol and 2 parts H_2O). After 10 min of stain, cells were washed twice and observed (Binns et al., 2006).

Transmission Electron Microscopy

Cells cultured in oleic acid containing media were prefixed (0.20 M PIPES, pH 6.8, 0.20 M sorbitol, 2.0 mM magnesium chloride, 2.0 mM calcium chloride, 4.0 % glutaraldehyde) for 5.0 minutes at room temperature, and for 72 hours in fresh prefix solution at 4.0 ºC. Samples were post fixed in 2.0 % potassium permanganate for 45 minutes, washed with water and incubated in 1.0 % uranyl acetate for 1.0 hour. Samples were washed three times before being dehaydrated in graded ethanol series (25 %, 50 %, 75 %, 95 % and 100 % ethanol) and daily infiltrations with increasing concentrations of Spurr's resin

(Wright, 2000). Samples were embedded in BEEM capsules and polymerized at 70 ºC. 80 nm thin sections were obtained, mounted on 200 mesh-grids and stained with uranyl acetate and lead citrate before images were obtained. Images were obtained with a JEOL 1200 EX electron microscope with a Sis Morda 11-mpixel side-mount CCD camera.

Cell Lysis and Organelle Fractionation

Cell pellets were first resuspended in100 OD_{600}/ ml of buffer containing 0.10 M Tris HCl pH 9.4 and 10 mM DTT for 5 minutes at room temperature. Cell pellet were then resuspended in yeast lyticase buffer (20 mM HEPES, pH 7.4 with Potassium Hydroxide, 50 mM Potassium Acetate, 200 mM sorbitol, 2.0 mM EDTA, 0.20 mM AEBSF, 1.0mM DTT and protease inhibitor cocktail: 0.2 mM 4-(2-aminoethyl) benzenesulfonyl fluoride hydrochloride, 1.2 µg/ml pepstatin A, 1.2 µg/ml leupeptin, 12 µg/ml p-toluenesulfonyl-L-arginine methyl ester, 12 µg/ml tosyl-lysyl-chloromethylketone, 12 µg/ml p-nitroenzoyl-L-arginine methyl ester, 12 µg/ml soybean trypsin inhibitor)). Samples were then treated with 4.0 mg of Zymolyase/ 1000 OD_{600} while in lyticase buffer for 45 minutes at 30 ºC. Samples were pelleted in a Beckman JA 17 rotor at 5500 rpm at 4.0 ºC for 5.0 minutes. Pellet was resuspended in lysis buffer (20 mM HEPES, pH 7.4, 200 mM sorbitol, 50 mM KOAc, 2 mM EDTA, and protease inhibitor cocktail), dounce homogenized and centrifuged in a Beckman JA 21 at 3000 rpm for 5.0 minutes at

4.0 ºC to obtain the post-nuclear supernatant (PNS). The PNS in yeast lysis buffer was loaded into a Beckman SW60 tube and layered with a 1 ml HEPES cushion (20 mM HEPES pH 7.4, 100 mM KCl, 2 mM $MgCl_2$) and centrifuged at 38,000 rpm for 1 hour at 4 °C in an SW60 rotor. Floating lipid droplet and membrane pellets were collected and taken through the lipid analysis.

Preparation of Samples for Lipid Analysis

For whole cell lipid analysis, yeast cell pellets were treated with Zymolyase 100T at 4 mg /1000 OD 600 for 40 minutes at 30 °C. Spheroplasts were weighed and resuspended with water to 0.45ml (For organelle fractions, protein concentration was determined with a Bradford assay). Lipids were extracted by a modified Bligh and Dyer Method (Bligh and Dyer, 1959) using 2.0 ml of ispropanol at 70 ºC for 30 minutes followed by 1.0 ml of chloroform. Lipids were extracted into chloroform and washed with 1.0 M KCl. Purified lipids were dried under Nitrogen gas and dissolved in 50 µl or 100 µl chloroform for TLC or mass spectrometric analysis respectively.

TLC Lipid Analysis

Extracted lipids in chloroform were spotted on 250 µm thick silica gel thin layer chromatography (TLC) plates (Whatman). After spotting, TLC plates were

treated with 3% cupric acetate, 8% phosphoric acid solution and lipid bands were digitally scanned and analyzed using ImageJ (v.1.41, NIH).

Mass Spectrometric Analysis

Samples subjected to mass spectrometric analysis were spiked with an internal standard mixture composed of 2 µg tri 15:0-TAG, 4 µg tri 21:0-TAG, 2 µg 13:0-cholesteryl ester, 4 19:0-cholesteryl ester. Samples were suspended in 0.4 ml of chloroform and fractionated by silica gel column chromatography (Supelco Discovery DSC-Si 6ml, 500 mg solid phase extraction (SPE) cartridges). Columns were pre-conditioned with hexane and lipids separated by sequential elution with solvents (hexane:diethyl ether [4:1, v/v], hexane:diethyl ether [1:1, v/v], methanol, and finally chloroform) (Laffargue et al., 2007). Solvents were evaporated off with N_2 prior to suspending neutral lipid in 0.1 ml chloroform. Neutral lipid fractions were diluted into chloroform-methanol [1:1, v/v] plus 10 mM aqueous ammonium acetate. Samples were introduced by direct infusion at a flow rate of 750 µl per hour into the electrospray source of a Waters Micromass Quattro Ultima Triple Quadrupole LC/MS/MS. TAGs and steryl esters (StE) were quantified in full-scan mode. Neutral loss scans for TAGs and StE were used separately to verify acyl-chain compositions and head group. The collision energies, with argon in the collision cell, were 20V for TAGs and StE. Full and neutral loss/precursor scans were acquired in continuum mode and averaged over

60 and 30 seconds, respectively. Conditions for acquisition were all under a positive capillary voltage of 3.50 kV, cone gas of 80 ml/hour, desolvation gas of 200 ml/hour, 80 °C source temperature and 200 °C desolvation temperature. The background of each spectrum was subtracted using a solvent blank, the peak areas integrated, isotopic overlap and response correction factors applied, and peaks quantified against their respective internal standards using in-house Visual Basic macros developed in Microsoft Excel.

Cell Lysis and Organelle Fractionation

Yeast microsomes were prepared as described (Brodsky et al., 1993) with few modifications. The post-nuclear supernatant in yeast lysis buffer (20 mM HEPES, pH 7.4, 200 mM sorbitol, 50 mM KOAc, 2 mM EDTA, and protease inhibitor cocktail: 0.2 mM 4-(2-aminoethyl) benzenesulfonyl fluoride hydrochloride, 1.2 µg/ml pepstatin A, 1.2 µg/ml leupeptin, 12 µg/ml p-toluenesulfonyl-L-arginine methyl ester, 12 µg/ml tosyl-lysyl-chloromethylketone, 12 µg/ml p-nitroenzoyl-L-arginine methyl ester, 12 µg/ml soybean trypsin inhibitor)) was loaded into a Beckman SW60 tube and layered with a 1 ml HEPES cushion (20 mM HEPES pH 7.4, 100 mM KCl, 2 mM $MgCl_2$) and centrifuged at 38,000 rpm for 1 hour at 4 °C in an SW60 rotor. Floating lipid droplet and membrane pellets were collected and taken through the lipid analysis procedure as described above.

Table 1. Plasmids and Yeast Strains Used in This Chapter

Plasmid	**Relevant characteristics**	**Source or reference**
pRS313	Ecoli/ yeast vector with *HIS3*	(Sikorski and Hieter, 1989)
pOA101	pRS313 containing *PAH1* 5' untranslated region (0.7kb), *PAH1* coding sequence (2.6kb), and 3'-untranslated region (0.5kb) inserted into Xho1/ SacII sites.	This study
pRS315	Ecoli/ yeast vector with *LEU2*	(Sikorski and Hieter, 1989)
pRS315-PGK	pRS315 containing PGK1 promoter and terminator	(Binns et al., 2006)
pRS315-PGK-CFP-HDEL	pRS315-PGK containing CFP-HDEL inserted into Xho1/ SacII sites	(Szymanski et al., 2007)
pRS316-PGK-CFP-HDEL	pRS316-PGK containing CFP-HDEL inserted into Xho1/ SacII sites	(Szymanski et al., 2007)
Strain	**Genotype** (all *Saccharomyces cerevisiae*)	
BY4742	Matα his3Δ1 leu2Δ0 lys2Δ0 ura3Δ0	Open Biosystems
BY4742-16601	BY4742 (*nem1Δ::Kan*^{r})	Open Biosystems
BY4742-10399	BY4742 (*spo7Δ::Kan*^{r})	Open Biosystems
BY4742-KS001	BY4742 (*pah1Δ::URA3*)	This study
SCY328	MATa ade2-1 his3-11,15 leu2-3,112,trp1-1ura3-1 can1	(Valachovic et al., 2006)
SCY2021	*dga1Δ::URA3, lro1Δ::URA3, are1Δ::LEU2, are2Δ::HIS3*	Gift from S. Sturley
OAS001	SCY328 (*pah1Δ::TRP1*)	This study
OAS004	*dga1Δ::URA3, lro1Δ::URA3, are1Δ::LEU2, are2Δ::HIS3, pah1Δ::TRP1*	This study

Results

Neutral lipid dyes stain the ER of *nem1Δ*, *spo7Δ* and *pah1Δ* mutants.

Previous studies at the Goodman lab demonstrated that BODIPY stained ring like structures that resembled the ER in *nem1Δ*, *spo7Δ* and *pah1Δ* mutants. By transforming these mutant cells with the ER lumenal marker CFP-HDEL, I was able to confirm that the BODIPY stained rings colocalized with the ER lumenal marker (Figure 2 A). This data suggests that neutral lipids may accumulate within the ER in the absence of *PAH1* or its protein phosphatases. Intrestingly, the prevalence of the BODIPY stained rings was much higher in *pah1Δ* mutants when compared to *nem1Δ* or *spo7Δ* mutants suggesting that Pah1p may still be partially active in the absence of Nem1p and Spo7p (Figure 2 B). Furthermore, a 63% decrease in lipid droplet number was observed in the *pah1Δ* when compared to wild-type suggesting a defect in lipid droplet biogenesis in the mutant (Figure 2 C).

Cell TAG is known to decrease in *pah1Δ* because *PAH1* encodes the main PA phosphatase that provides its precursor, DAG (Han et al., 2006). To determine whether the decrease in lipid droplets in *pah1Δ* can be attributed to an overall decrease in neutral lipids, TAG and StE levels were measured in the mutant and compared to wild-type. As expected, there was a decrease in TAG in *pah1Δ* cells

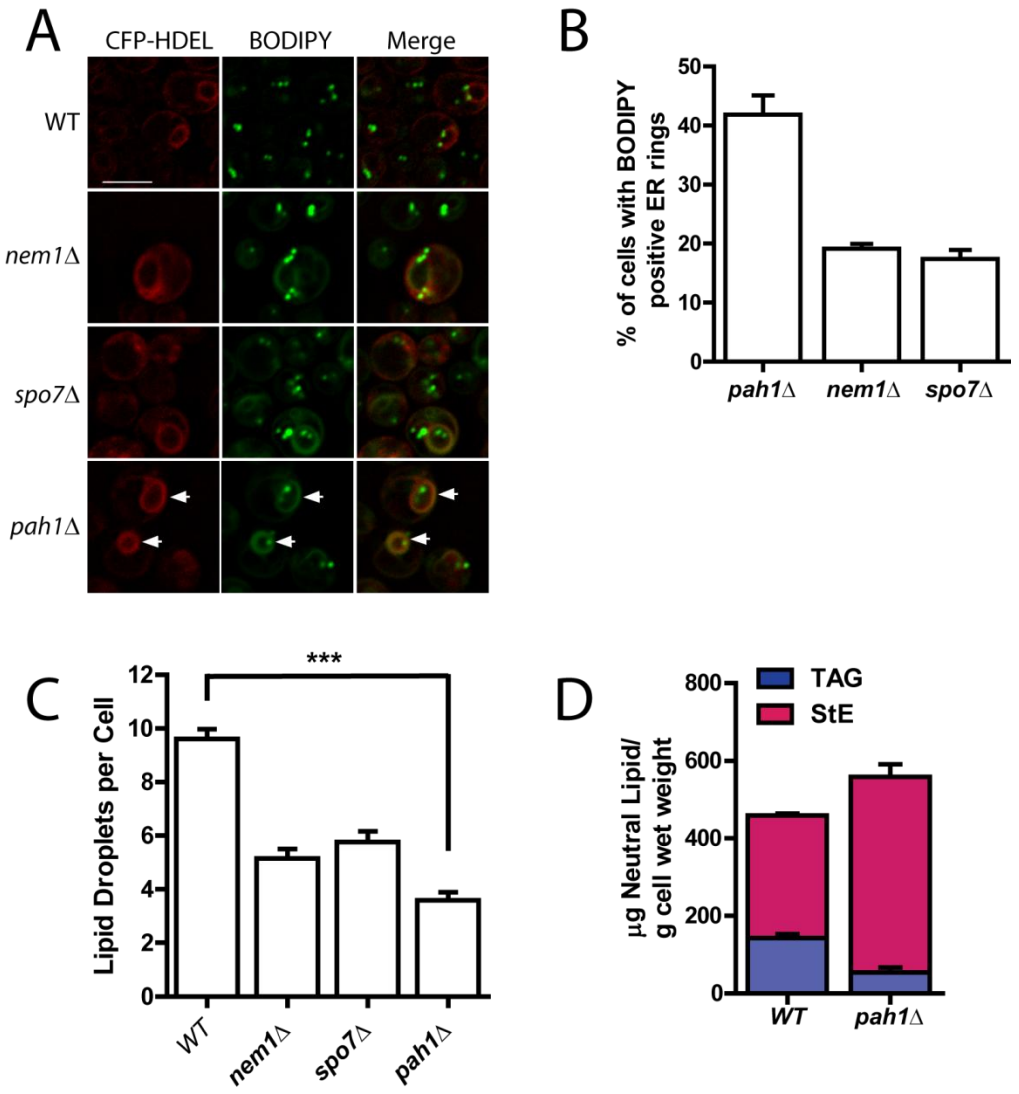

Figure 2. *pah1Δ* has fewer lipid droplets but a similar amout of neutral lipid. (A) BODIPY-stained ER rings. Fluorescence images of cells of the indicated strains containing the ER marker CFP-HDEL, which were cultured in minimal dextrose medium (SD) and stained with BODIPY. Note the fewer droplets in *pah1Δ*. Scale bar, 5 µm. (B) Histogram showing percentage of cells with BODIPY positive ER rings for the indicated yeast strains. (C) Comparison of droplet number in WT, *nem1Δ, spo7Δ* and *pah1Δ* cells. ***p<.0001 over, droplets in cells (examining z-section series) from four independent experiments, at least 20 cells per field, SE shown. (D) Total neutral lipid content from mass spectrometry. Means and ranges are shown from two independent experiments.

but a compensatory increase in StE was also observed so that the sum of the two neutral lipid classes, which normally are packaged into droplets, was at least as high in the *pah1Δ* mutant (Figure 2 D). These results demonstrate that the decrease in lipid droplet number observed in the *pah1Δ* mutant cannot be attributed to a decrease in overall neutral lipid.

As mentioned earlier, the absence of *PAH1* results in nuclear/ ER membrane proliferation that is due to a de-repression of phospholipid biosynthesis, causing nuclear envelope deformation and the appearance of ER stacks (Santos-Rosa et al., 2005). To determine whether the BODIPY stained rings in *pah1Δ* might be a result of altered ER morphology rather than neutral lipid accumulation, cells disrupted in both *PAH1* and all four acyltransferases for the generation of TAG and StE (*DGA1*, *LRO1*, *ARE1* and *ARE2* (Oelkers et al., 2002; Petschnigg et al., 2009)) were stained with three widely used neutral lipid dyes (BODIPY 493/503, Nile Red and Oil red O). BODIPY weakly stained the cytosol in the acyltransferace deficient 'quad' mutant (Figure 3 A, 4KO). In contrast, membrane rings were observed (albeit with reduced intensity when compared to *pah1Δ* alone) when *PAH1* was additionally knocked out, generating the 'quint' mutant (Figure 3 A, 5KO). These data suggest that BODIPY 493/503 cannot be used to effectively detect membrane neutral lipids in *pah1Δ*, because it stains membrane stacks devoid of neutral lipid.

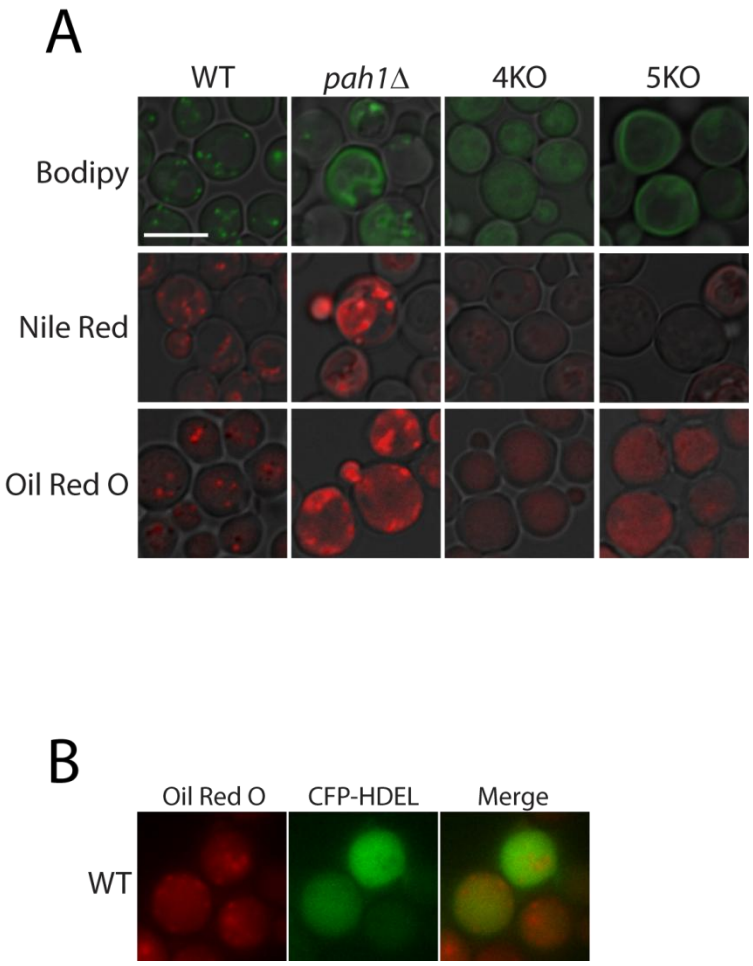

Figure 3. Neutral lipid dyes do not stain lipid droplets exclusively in *pah1Δ*. (A) BODIPY, Nile Red and Oil Red O staining of wild type, *pah1Δ*, 4KO (*dga1Δ lro1Δ are1Δ are2Δ*) and 5KO (*pah1Δ dga1Δ lro1Δ are1Δ are2Δ*) strains grown in SD medium. Images incorporate both brightfield and fluorescent channel for the indicated lipophilic dyes. Scale bar, 5 μm. (B) Isopropanol fixation alters ER membrane morphology (green).

Nile Red like BODIPY, also stained membranes of some cells of the 'quint' mutant. In contrast, Oil Red O, a dye traditionally used to stain neutral lipids in plants and animals did not stain membranes of the 'quint' mutant at all, but the isopropanol fixation required for staining cells with Oil Red O destroys membrane morphology (Figure 3 B).

Neutral lipids accumulate in the ER in the absence of *PAH1*

To gain better evidence of ER accumulation of neutral lipids in *pah1Δ*, the mutant was cultured in oleic acid-containing media to stimulate neutral lipid synthesis. Culturing in oleic acid resulted in an increase in occurrence and severity of the BODIPY-stained ER phenotype compared to mutants grown in SD media (Figure 4 A). By transmission electron microscopy, wild-type cells had large lipid droplets identified as round electron transparent structures that were absent in the 'quad' mutant strain (Figure 4 B). The proliferated ER was clearly seen in *pah1Δ*, and the membrane stacks contained many electron transparent inclusions consistent with neutral lipid within this compartment. Sometimes, larger inclusions were seen within proliferated ER as if tiny lipid droplets had coalesced (Figure 5). The bilayer structure could not be clearly visualized adjacent to the inclusions and it was impossible to verify whether the inclusions were between leaflets of the bilayer. Nevertheless, these membrane inclusions were entirely absent in the proliferated ER of the 'quint' mutant (Figure 4 B).

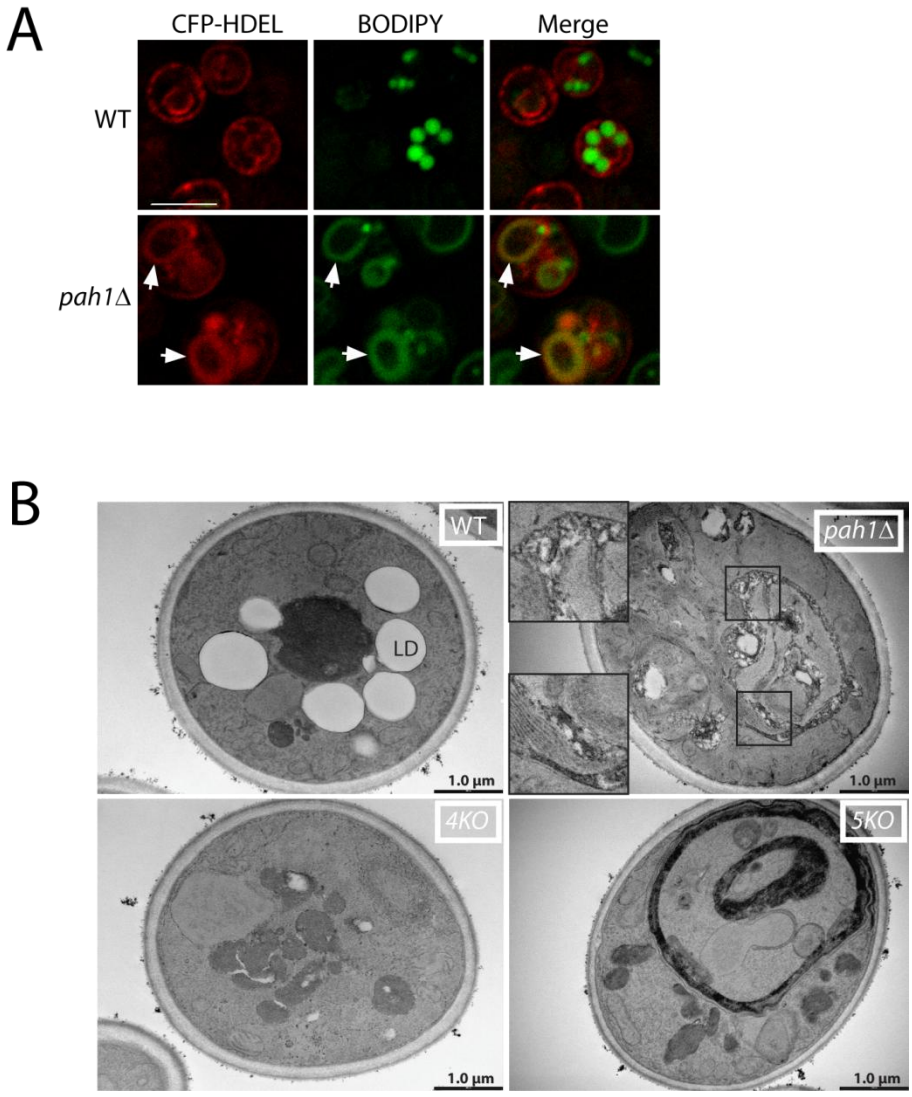

Figure 4. Neutral lipids accumulate in the ER in the absence of *PAH1*. (A) BODIPY (green) stained ER (red) phenotype (arrows) is more severe when cells are cultured in oleic acid containing media. Scale bar, 5 µm. (B) Inclusions in *pah1Δ* membranes seen with transmission electron microscopy. The indicated strains were cultured overnight in oleic acid medium prior to fixation. For *pah1Δ* inserts at higher magnification of boxed areas are shown to illustrate membrane inclusions. Note the membrane proliferation but no inclusions in the 5KO stain. LD: Lipid Droplet.

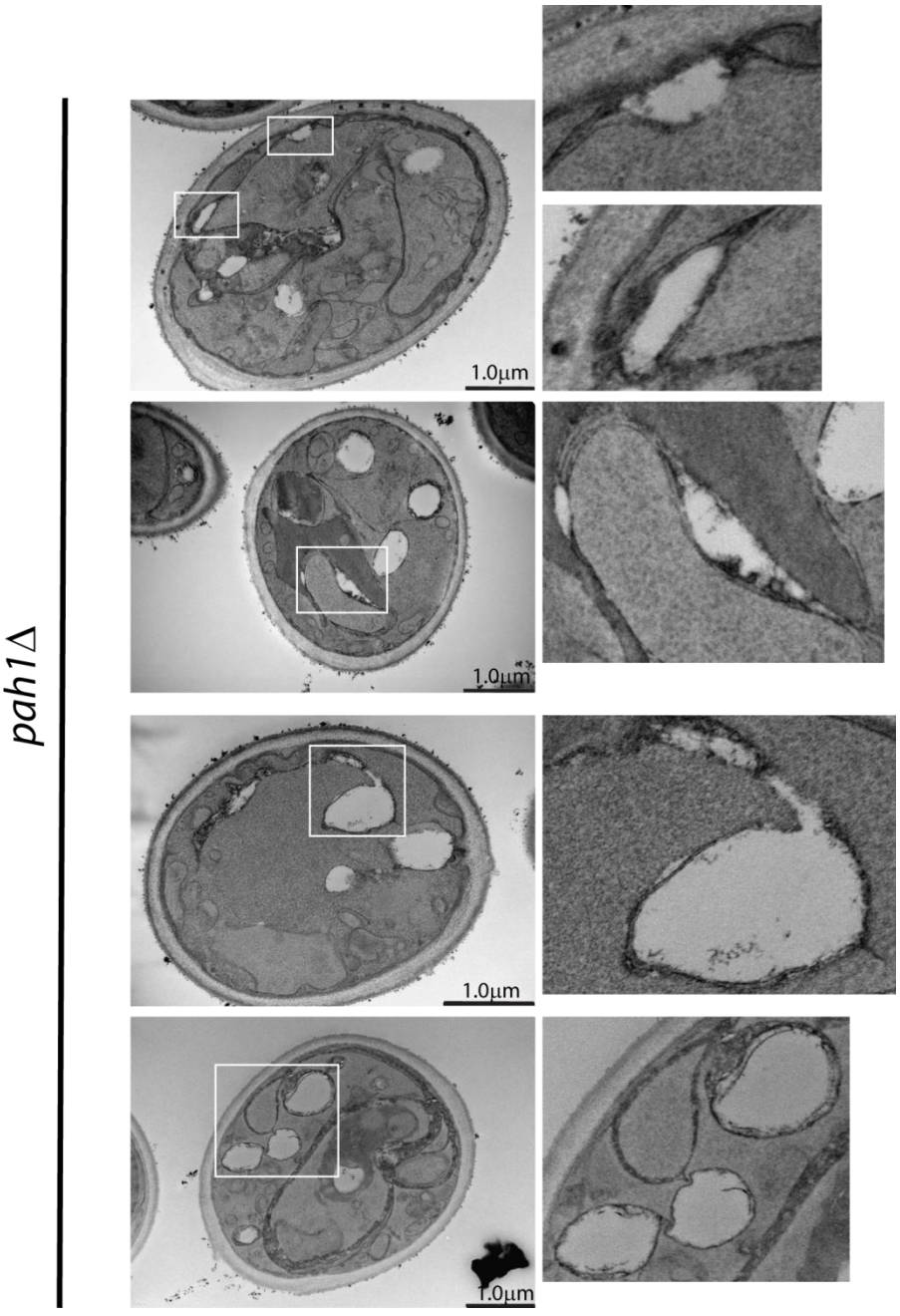

Figure 5. Electron micrographs of *pah1Δ* cells demonstrating large neutral lipid inclusions in membranes. Cells were cultured overnight in oleic acid medium. The images in the right column are enlarged sections of the images in the left column

This data shows that neutral lipids do accumulate within the ER of the *pah1Δ* mutant, and demonstrates that an increase in neutral lipid synthesis correlates with an increase in ER neutral lipids of the *pah1Δ* mutant.

To biochemically verify membrane accumulation of neutral lipids in *pah1Δ*, cellular membranes and lipid droplets were separated by ultracentrifugation from post nuclear supernatants of wild-type and *pah1Δ* cells cultured in oleic acid. In wild-type cells, 10.2 % of TAG was found in the membrane fraction (Figure 6 A). In contrast, 22.0 % of TAG was found in membranes of *pah1Δ* cells, although the absolute amount of TAG in membranes was actually decreased 28.0 % in the mutant. This data suggests that the neutral lipid membrane inclusions observed in *pah1Δ* were not likely TAG. In contrast, there was 5.2 times more membrane associated StE in *pah1Δ* compared to wild-type (Figure 6 B).

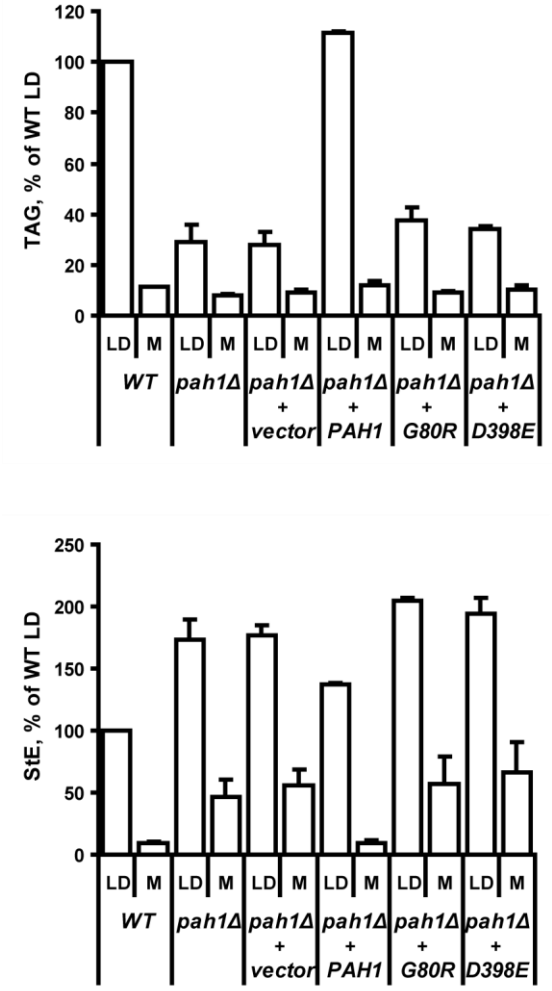

Figure 6. Isolated membranes of *pah1Δ* contain more steryl esters. Droplet and membrane levels of TAG (top) and StE (bottom) in the indicated strains. Post-nuclear extracts from spheroplasts (grown in oleate) were fractionated by centrifugation. An identical percentage of the floating droplets and membrane pellets, normalized to total protein in the extracts, were subjected to TLC. Error bars indicate the range of values from two independent experiments.

Discussion

The current model for droplet biogenesis suggests that the neutral lipids within droplets originate from the ER because: (1) the neutral lipid synthesizing enzymes are located on the ER, (2) of the presence of ER proteins on droplets and (3) of the observed physical association of droplets with the ER. The presence of neutral lipid (electron transparent inclusions) within the ER of *pah1Δ* supports the notion of droplets originating from the ER, and suggests that the ER (although abnormal in *pah1Δ*) has the capacity to store a certain amount of neutral lipid before they are transferred into droplets. Biochemical analysis of *pah1Δ* membranes also demonstrated an increase in membrane StE supporting the neutral lipid identity of the electron transparent inclusions (Figure 6). It is likely that the total *pah1Δ* membrane neutral lipid levels are underestimated because of the high centrifugal force used to separate droplets from membranes. This high force may also remove neutral lipid stored in membranes of the *pah1Δ* mutant.

Although electron transparent inclusions (possibly neutral lipid inclusions) were observed within ER membrane stacks, I was unable to determine precisely whether these inclusions were between membrane phospholipid monolayers. This proved to be difficult because of the disorganized nature of membrane stacks with neutral lipid inclusions, and the lack of understanding of phospholipid organization within the stacks. Viewing neutral lipid inclusions within ER stacks

by electron tomography may provide a better understanding on the organization of the membranes with neutral lipids.

It is interesting that the BODIPY stained ER rings were less frequent in the *nem1Δ* and *spo7Δ* mutants compared to *pah1Δ.* Also, there were more lipid droplets in the protein phosphatase mutants than *pah1Δ* (Figure 2 C). This indicates that Pah1p could retain some of its in vivo PAP activity when a member of the Nem1p/ Spo7p phosphatase complex is absent. Another possibility is the availability of other proteins that could supplement for the loss of either member of the Nem1p/ Spo7p phosphatase complex, however, no such protein phosphatase has been discovered to date.

The abnormal lipid droplet morphology observed in *pah1Δ* mutants is consistent with data showing that lipin mutant mice have immature adipocytes (obtained from epididymal fat pads) with small and heterogeneous lipid droplets rather than the large unilocular droplets observed in wild-type tissues (Peterfy et al., 2001). However, the availability of multiple lipin protein isoforms in mammals with different tissue expression patterns and functions makes it difficult to compare morphological abnormalities to the yeast mutant.

CHAPTER 3

Pah1p AND STERYL ESTERS IN COMBINATION ARE ESSENTIAL FOR LIPID DROPLET FORMATION

Introduction

Neutral lipids within the lipid droplet core are hypothesized to be stored in an organized manner consisting of several ordered steryl ester shells below the phospholipid monolyayer, and TAG randomly stored at the center (Czabany et al., 2008). Lipid droplets will assemble if either TAG or StE alone is the only neutral lipid available. However, the protein composition between TAG only and StE only containing droplets vary, suggesting that the neutral lipid composition of a lipid droplet can affect the protein recruitment to these organelles (Czabany et al., 2008).

In the absence of *PAH1*, total neutral lipid levels were not significantly altered, however, the ratio of TAG to StE was altered when compared to wild-type (Figure 2 D). As expected, TAG levels in *pah1Δ* were lower than wild-type, but a compensatory increase in *pah1Δ* StE levels was observed. Lipid droplets are generally assumed to contain both TAG and StE, but it is unknown whether independent machineries exist for shuttling these neutral lipids into droplets, or whether an individual droplet can contain exclusively TAG or StE. The goal of

this chapter was to determine whether Pah1p was particularly important in shuttling individual neutral lipid classes (TAG or StE) into lipid droplets.

Materials and Methods

Strains and Culture Conditions

All yeast strains and plasmids used in this chapter are listed in Table 2. Cells were cultured as described in Chapter 2

Fluorescence Microscopy

Images were acquired as described in Chapter 2. For time course (Figure 7 C), BODIPY stained cells placed under a microscope cover slip were observed at 10 minutes and two 20 minute time points.

Table 2: Yeast Strains Used in This Chapter

Strain	**Genotype** (all *Saccharomyces cerevisiae*)	**Source or Reference**
SCY328	MATa ade2-1 his3-11,15 leu2-3,112,trp1-1ura3-1 can1	(Valachovic et al., 2006)
SCY1998	*dga1Δ::URA3, lro1Δ::LEU2*	Gift from S. Sturley
SCY1703	*are1Δ::HIS3, are2Δ::LEU2*	Gift from S. Sturley
SCY2021	*dga1Δ::URA3, lro1Δ::URA3, are1Δ::LEU2, are2Δ::HIS3*	Gift from S. Sturley
OAS001	SCY328 (*pah1Δ::TRP1*)	This study
OAS002	*dga1Δ::URA3, lro1Δ::LEU2, pah1Δ::TRP1*	This study
OAS003	*are1Δ::HIS3, are2Δ::LEU2, pah1Δ::TRP1*	This study

Results

Knockout of *PAH1* and steryl esters in combination abolishes lipid droplets in cells grown in glucose media.

To address whether Pah1p was particularly important for the packaging of TAG vs StE, I knocked out *PAH1* in cells that either lacked the genes for the two DAG acyltransferases (*DGA1* and *LRO1*) or for the two steryl acyltransferases (*ARE1* and *ARE2*). As reported previously (Garbarino et al., 2009), lipid droplets form in the absence of TAG or StE, although the numbers are reduced slightly in the absence of steryl acyltransferases and more significantly in the absence of DAG acyltransferases (Figure 7 A and B). These data indicate that neither TAG nor StE formation is absolutely essential for lipid droplet formation. When *PAH1* is additionally knocked out in the background of cells lacking the DAG acyltransferases, there was a small (26 %) but highly reproducible decrease in droplet number, even though there was no significant decrease in total StEs for this strain (Figure 7). In contrast, no droplets were detected when *PAH1* was disrupted in the *are1Δ are2Δ* background, even though this strain contained about as much TAG as wild-type (Figure 7). These data suggest that in the absence of StE synthesis, Pah1p is required to form droplets containing TAG, at least when the cells are cultured in glucose media.

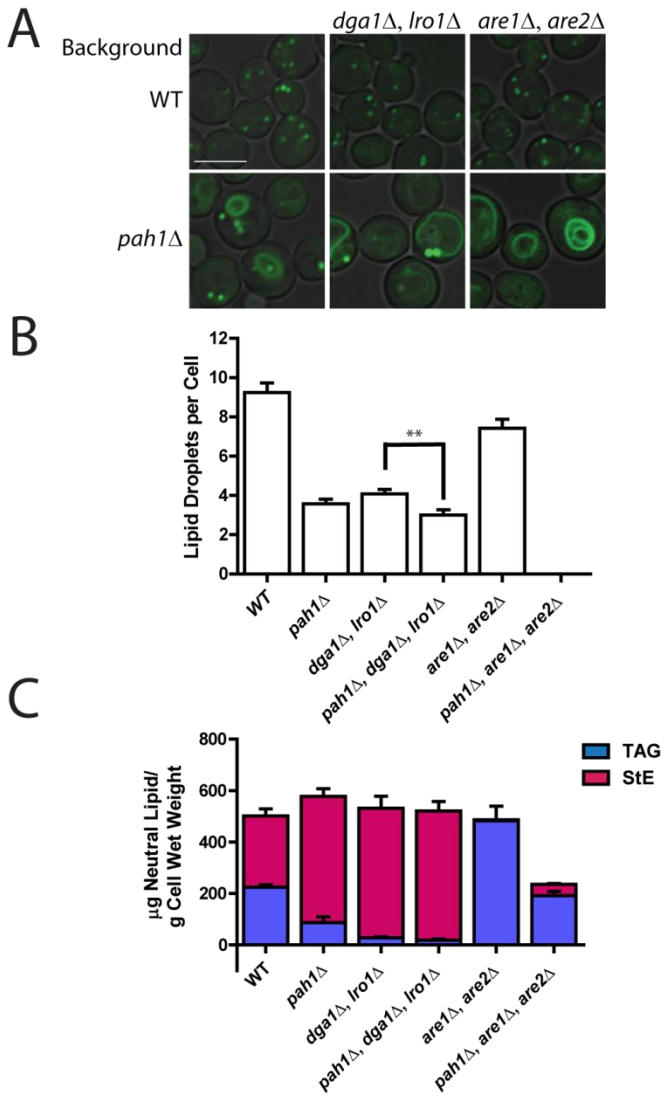

Figure 7. Knockout of *PAH1* and sterol acyltransferases abolishes lipid droplets in cells grown in SD. (A) BODIPY staining of the indicated strains in SD. *DGA1* and *LRO1* encode DAG acyltransferases, *ARE1* and *ARE2* encode steryl acyltransferases. Images incorporate both brightfield and FITC channel (for lipid droplets). Scale bar, 5 µm. (B) Lipid droplet number in strains shown in 'A.' Droplets in approximately 30 cells were counted in z-section series from three independent experiments. Mean ± SE shown. Knockout of *PAH1* always resulted in significantly lower droplets, although the significance in only the middle pair is shown for clarity, **, $p<0.001$. (C) Quantification of TAG and StE from MS analysis for the indicated strains grown in SD. Means and ranges from two independent experiments are shown.

The lack of lipid droplets in the *pah1Δ are1Δ are2Δ* mutant was dependent on media and growth conditions. I observed that when this strain is cultured in oleic acid-containing medium, the large fatty acid load resulted in a few lipid droplets but, they were much fewer in number when compared with *pah1Δ* (Figure 8 A and B). Furthermore, lipid droplets assembled when this mutant is removed from normal laboratory yeast culturing conditions. When the *pah1Δ are1Δ are2Δ* mutant culture was placed on a lab bench or under a microscope cover slip for a period of time lipid droplets start to form from cells that originally did not have any (Figure 8 C). These data indicate that the lack of lipid droplets in the *pah1Δ are1Δ are2Δ* mutant is not absolute. It suggests that environmental factors can influence lipid droplet biogenesis, at least in this triple mutant.

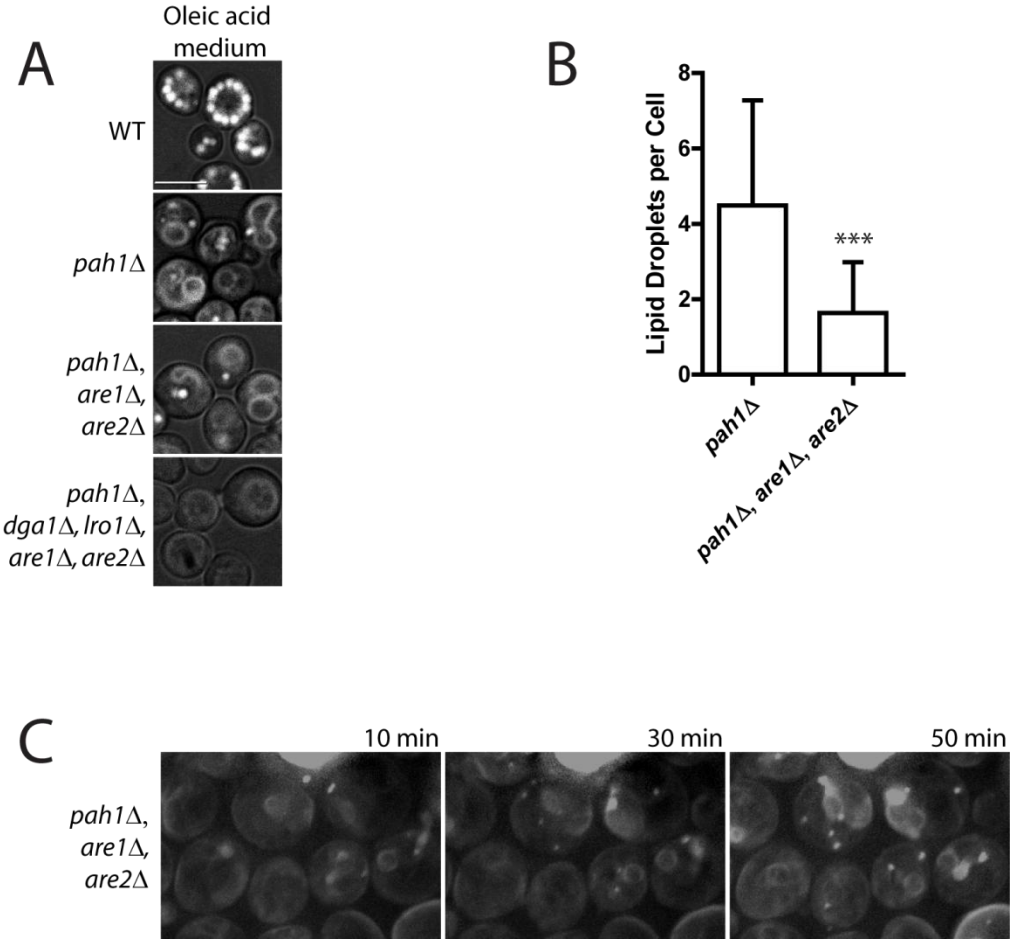

Figure 8. Lipid droplet formation in the absence of Pah1p and sterol acyltransferases. (A) BODIPY staining of the indicated strains grown in medium containing oleic acid. (B) A comparison of droplet number in *pah1Δ* and *pah1Δ are1Δ are2Δ* grown in oleic acid. Error bars represent SD; ***, p<0.0001. (C) BODIPY stained lipid droplets assemble in the *pah1Δ are1Δ are2Δ* mutant. Projection images for the indicated time points are shown.

Discussion

The inability of cells to form lipid droplets in the absence of StE synthesis and *PAH1* in glucose grown cells was surprising. One explanation could be that the absence of *PAH1* combined with an accumulation of unesterified sterols may stiffen the membrane (Bacia et al., 2005), preventing droplet formation. Another possibility is that there is a threshold of total cell neutral lipids that has to be reached before a droplet can form and, the fact that the sum of TAG and StE in the *pah1Δ are1Δ are2Δ* (which is about half of that in the other strains) may be below this threshold.

Another explanation for the lack of droplets in the *pah1Δ are1Δ are2Δ* mutant could be that it is due to severe alterations to components involved in the biogenesis of two types of droplets. StE containing droplets would obviously be shutdown because of the lack of sterol acyltransferases, while the assembly of TAG containing droplets is defective due to the absence of Pah1p. This explanation is supported by the presence of wild-type levels of TAG but no droplets in the mutant, and the increased StE content in lipid droplet fractions from *pah1Δ*. However, it is contradicted by the fact that lipid droplet fractions of *pah1Δ* still contain about 30 % of wild-type TAG and even fewer in membranes (Figure 6). Perhaps the wild-type levels of TAG in the *pah1Δ are1Δ are2Δ* mutant is obtained from increased DAG acyltransferase activity, or from DAG generated via increased phospholipid lipolysis or through increased activity of the other

phosphatidic acid hydrolases. The magnesium-independent phosphatidic acid hydrolases Dpp1p and Lpp1p are localized to the vacuole and Golgi compartments of cells respectively (Han et al., 2004; Han et al., 2001; Huh et al., 2003). If they contribute to TAG synthesis in the *pah1Δ are1Δ are2Δ* mutant, it would be interesting to observe what organelle droplets in this mutant originate from. It will not be unusual for lipid droplets to originate from vacuoles, because this has been observed in certain mutants (Gaspar et al., 2008). The other phosphatase candidate is a magnesium-dependent one whose identity is yet to be established (Han et al., 2006).

The fact that droplets barely form in the *pah1Δ are1Δ are2Δ* mutant unless stressed is very appealing because: (1) The presence of wild-type levels of TAG in the mutant further confirms that the ER has the capacity to store neutral lipids, and (2) It suggests that Pah1p independent pathways may exist to regulate lipid droplet formation. Under normal yeast culturing conditions the pathways for droplet formation (which may involve Pah1p and the StE synthesis) may be inhibited in the *pah1Δ are1Δ are2Δ* mutant. However, environmental stressors to which the mutant is subjected may stimulate droplet formation. Cells at room temperature are in a condition about 5.0 ºC below what is required for optimal growth and those under a microscope cover slip or in a culture flask (out of the laboratory shaker) for long periods are subjected to hypoxic conditions. Interestingly, ER stress and hypoxia are both known to individually induce lipid

droplet accumulation in yeast and mammalian tissue cultures, but the mechanisms that regulate droplet formation under these conditions remain unknown (Fei et al., 2009; Gordon et al., 1977).

CHAPTER 4

EVIDENCE THAT DIACYLGLYCEROL IS IMPORTANT FOR LIPID DROPLET FORMATION

Introduction

Pah1p activity is negatively regulated through phosphorylation by Cdc28p kinase. It is dephosphorylated via the membrane associated protein phosphatase complex Nem1p/ Spo7p. The dephosphorylation of Pah1p enhances its activity and exposes an amino-terminal amphiphatic helix that allows Pah1p to interact with the ER membrane, where it converts PA into DAG. DAG can then be used to synthesize triglycerides or it can be converted back to PA via the diacylglycerol kinase Dgk1p (Figure 1).

The absence of *PAH1* results in alterations to individual amounts of phospholipids including the expected decrease in DAG and concomitant increase in PA (Han et al., 2006). DAG is a lipid that is well known to physically perturb phospholipid bilayers and promote high curvature of leaflets (Carrasco and Merida, 2007; Goñi and Alonso, 1999). It also assists in budding and fusion of vesicles from Golgi complex membranes (Asp et al., 2009; Roth, 1999).

In this chapter, I show that the phosphatidic acid hydrolase activity of Pah1p is required for efficient droplet formation, and I provide evidence for the

involvement of diacylglycerol in the same process as well. Finally, I suggest a model for nascent droplet formation that involves the unique localization of Nem1p and Spo7p.

Materials and Methods

Strains and Culture Conditions

All yeast strains used in this chapter are listed in Table 3.

All cells were cultured as described in chapter 2 except for YJP1078 and OAS008 which were cultured in Synthetic Complete Dextrose media (SCD) which included 2.0 % glucose, Yeast Nitrogen Base and required amino acid dropout mix. For induction of Dga1p expression in OAS008 strain, SC-Dextrose cultured cells at stationary phase growth was diluted to 0.25 OD_{600}/ ml in SC-Raffinose. After about 20 hours, samples were diluted to 0.5 OD_{600}/ml in SC-Galactose and allowed to grow for 2.0 hours before being prepared for microscopic observation.

Fluorescence Microscopy

All Images were acquired as described in Chapter 2.

For time course (Figures 15-18), samples in SC-Galactose were stained with BODIPY for 5 minutes and 7.0 OD_{600} units was pelleted and resuspended in 50 µl of its media. 5.0 µl of resuspended pellet was transferred to a glass bottom culture dish (MatTek corporation) and layered with SC-Galactose containing 1.0 % Bacto Agar at 40 ºC and BODIPY. Finally, the glass bottom culture dish with samples under an agar pad was layered with 2.0 ml of SC-Galactose medium containing BODIPY. Images were obtained every 15 minutes.

For Figure 14, membrane pellets of the required yeast strain were resuspended gently in 0.5 ml lysis buffer and stained for 10 minutes with BODIPY 493/503 before observation by fluorescence microscopy.

Three-dimensional reconstruction (Figure 13) was performed using Imaris software (Bitplane AG, Zurich, Switzerland).

DNA Manipulations

All plasmids used in this study are listed in Table 3. Site-directed mutations to plasmids were performed using the QuikChange site-directed mutagenesis kit (Stratagene). *PAH1* knockout in OAS001, OAS002 and OAS003 strains was performed by homologous recombination using a DNA cassette containing ~500 bp of *PAH1* sequence (from the 5' and 3' untranslated region flanking *PAH1* ORF) ligated to opposite ends of a *TRP1* sequence. BY4742-SL001 strain was generated by homologous recombination with the use of a DNA cassette containing mCherry, followed by the *PGK1* 3' terminator and *URA3* to the 3' end of the *NEM1* ORF. OAS008 strain was generated by homologous recombination with the use of a DNA cassette containing tdTomato, followed by the *PGK1* 3' terminator and Hygromycin cassette to the 3' end of the *NEM1* ORF .Yeast strains were transformed by the lithium acetate method (Ito et al., 1983). DNA manipulations resulting in changes to coding sequence as well as changes to genome were verified by sequence performed by the McDermott Center for

Human Growth and Development (University of Texas Southwestern Medical Center, Dallas, TX).

Table 3. Plasmids and Yeast Strains Used in This Chapter

Plasmid	**Relevant characteristics**	**Source or reference**
pRS313	Ecoli/ yeast vector with HIS3	(Sikorski and Hieter, 1989)
pOA101	pRS313 containing *PAH1* 5' untranslated region (0.7kb), *PAH1* coding sequence (2.6kb), and 3'-untranslated region (0.5kb) inserted into Xho1/ SacII sites.	This study
pOA102	pOA101 containing G80R mutation in PAH1 coding sequence	This study
pOA103	pOA101 containing D396E mutation in PAH1 coding sequence	This study
pOA104	pOA101 containing D400E mutation in PAH1 coding sequence	This study
pRS315	Ecoli/ yeast vector with LEU2	(Sikorski and Hieter, 1989)
pRS315-PGK	pRS315 containing PGK1 promoter and terminator	(Binns et al., 2006)
pRS315-PGK-CFP-HDEL	pRS315-PGK containing CFP-HDEL inserted into Xho1/ SacII sites	(Szymanski et al., 2007)
pRS316-PGK-CFP-HDEL	pRS316-PGK containing CFP-HDEL inserted into Xho1/ SacII sites	(Szymanski et al., 2007)
pRS314-GAL10	pRS314 containing GAL10 promoter and PGK1 terminator	This study
DB001	pRS314-GAL10 containing DGA1 inserted into BamHI and HindIII sites	This study
Strain	**Genotype** (all *Saccharomyces cerevisiae*)	
BY4742	Matα his3Δ1 leu2Δ0 lys2Δ0 ura3Δ0	Open Biosystems
BY4742-SL001	BY4742 strain with mCherry at the c-terminus of the *NEM1* ORF	This study
BY4742-KS001	BY4742 (*pah1Δ::URA3*)	This study
SCY328	MATa ade2-1 his3-11,15 leu2-3,112,trp1-1ura3-1 can1	(Valachovic et al., 2006)
SCY1998	*dga1Δ::URA3, lro1Δ::LEU2*	Gift from S. Sturley
OAS001	SCY328 (*pah1Δ::TRP1*)	This study
OAS005	SCY328 (*dgk1Δ::HIS3*)	This study
OAS006	SCY328 (*dgk1Δ::HIS3, pah1Δ::TRP1*)	This study
OAS007	SCY1998 (*dgk1Δ::HIS3*)	This study
YJP1078	MATα, *his3Δ*0, l*eu2Δ*0, *lys2Δ*0, *ura3Δ*0, *are1Δ*::kanMX, *are2Δ*::kanMX, *dga1Δ*::kanMX, *lro1Δ*::kanMX	(Gaspar et al., 2011)
OAS008	YJP1078 strain with tdTomato at the c-terminus of the *NEM1* ORF	This study

Results

Phosphatase activity of Pah1p is required for the efficient formation of lipid droplets

It has previously been shown that the PA phosphatase activity of Pah1p depends on an intact amino-terminal lipin homology domain and haloacid dehalogenase domain of the protein (Figure 9 A) (Han et al., 2007; Han et al., 2006). To determine whether the low-droplet number phenotype of *pah1Δ* is caused by the absence of catalytic activity itself, I generated three point mutants that are known to disrupt the catalytic activity of the protein. The *pah1Δ* strain was then transformed with plasmids encoding wild-type or mutated Pah1p. Although the wild-type copy of Pah1p was able to revert both the BODIPY-stained ER rings (Figure 9 B) and lipid droplet phenotypes (Figure 9 C) to wild-type, none of the three point mutants were able to complement the *pah1Δ* strain. Similarly, only the wild-type allele was able to reverse the accumulation of StE in isolated membrane fractions (Figure 6). This data demonstrates the importance of the PA phosphatase activity of Pah1p for efficient lipid droplet formation.

The importance of diacylglycerol in lipid droplet formation

Data generated thus far suggest that DAG generated by Pah1p could be important for droplet formation. This is consistent with a study showing that manipulation of DAG levels in mammalian cells affects lipid droplet assembly

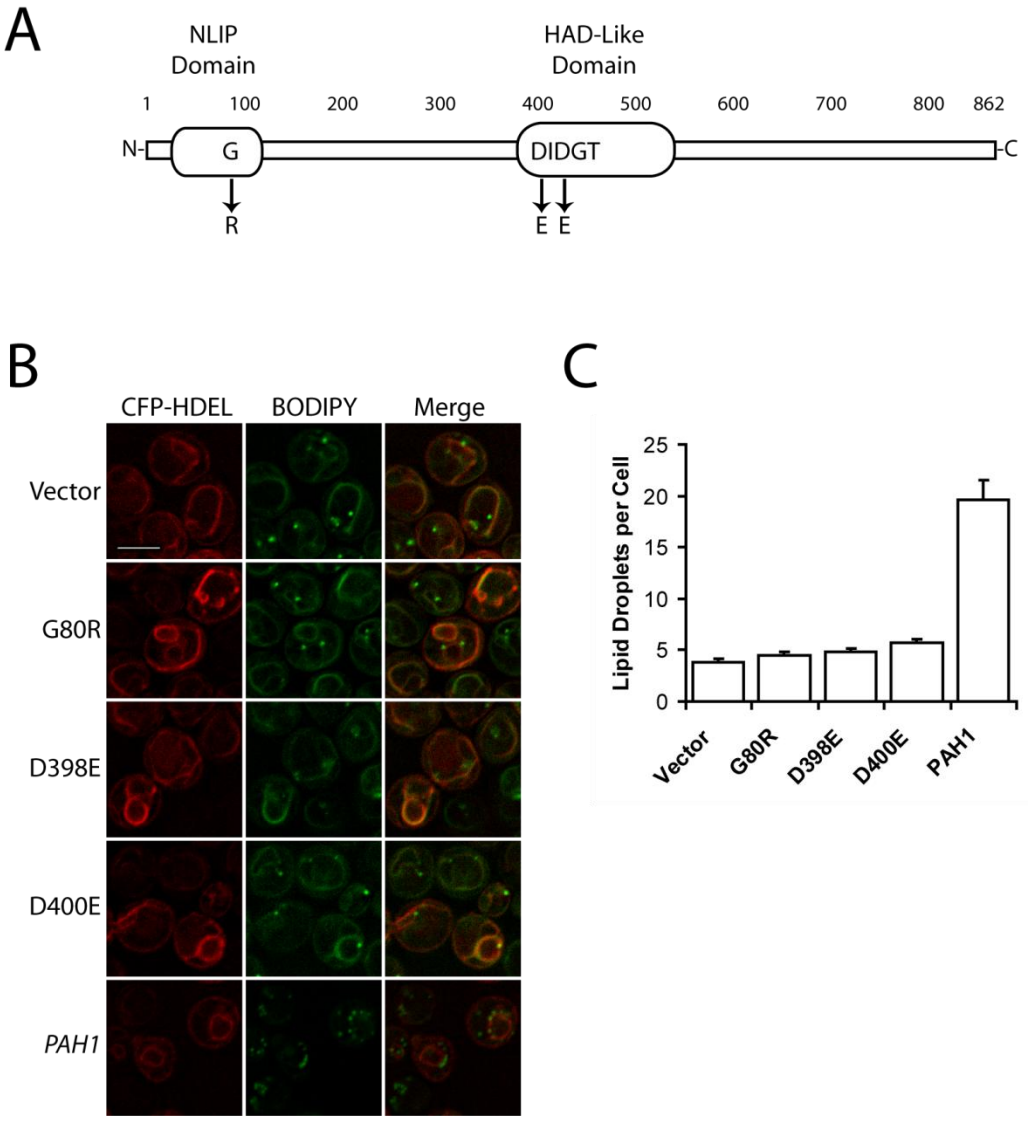

Figure 9. Phosphatidic acid phosphatase activity of Pah1p is required for efficient formation of lipid droplets. (A) Diagram of Pah1p primary structure. (B) The *pah1Δ* strain expressing the indicated *PAH1* alleles on a pRS313 vector. The ER marker CFP-HDEL was expressed on a plasmid and driven by the PGK1 promoter. Lipid droplets were stained with BODIPY. Cells were observed in SD medium. Scale bar, 5 μm. (C) Droplet number per cell in strains shown in 'B.'

(Skinner et al., 2009). If DAG is required for droplet formation, then overproducing DAG may be able to bypass the role of Pah1p. To test this idea, DAG synthesis was increased by eliminating the backward reaction to PA in a DAG kinase knockout strain, *dgk1Δ*. Dgk1p has recently been shown to provide PA for phospholipid synthesis during lag phase of growth (Fakas et al., 2011). The expected increase in DAG and decrease in PA for the *dgk1Δ* mutant was confirmed as has been previously reported (Figure 10 D) (Fakas et al., 2011; Han et al., 2008b). As predicted, the *dgk1Δ* strain alone had significantly more lipid droplets than wild-type (Figure 10 A and B), which were often arranged as "pearls on a string" (defined as four or more lipid droplets in a row spaced ≤ 0.5 μm apart) on the perinuclear ER (Figure 10 A, arrows). Furthermore, a knockout of *PAH1* in the *dgk1Δ* background increased lipid droplet number when compared to *pah1Δ* alone. This data indicates that the increase in DAG generated by Pah1p facilitates lipid droplet formation, but with the *pah1Δ dgk1Δ* strain DAG (likely generated by another Mg^{2+} dependent PA phosphatase activity whose identity has not yet been established (Han et al., 2006)) bypasses the role of Pah1p in droplet formation (Figure 10 A and B).

Accumulation of DAG in the *dgk1Δ* strain would be expected to result in increased TAG synthesis and a subsequent increase in lipid droplet formation. To determine if this was the case, *DGK1* was knocked out in a strain

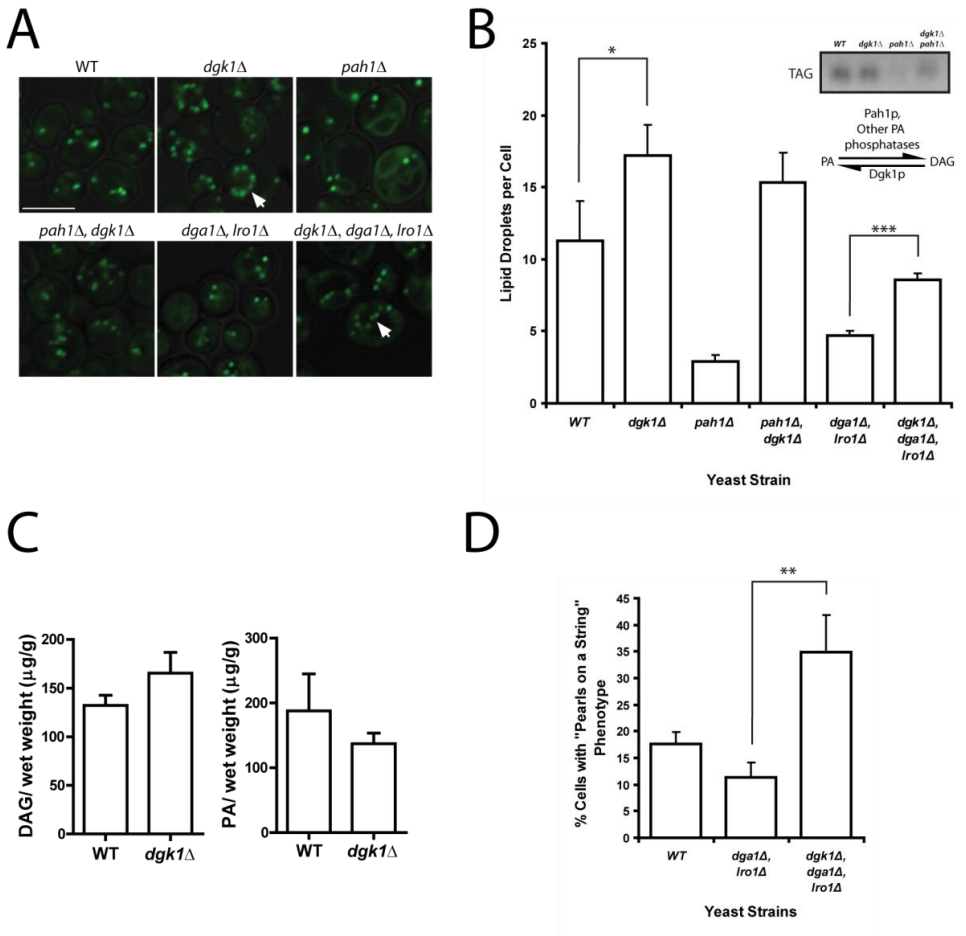

Figure 10. Knockout of DAG kinase leads to more droplets and a bypass in Pah1p function. (A) Knockout of *DGK1* increases droplet number independent of TAG. The indicated strains were grown in SD and lipid droplets were stained with BODIPY. Images incorporate brightfield channel. Scale bar, 5 μm. Arrows illustrate "pearls on a string" phenotype. (B) Droplet number increases in *dgk1Δ* even in the absence of TAG. Inset shows TAG levels in the indicated mutants and illustrates the enzymes that catalyze PA-DAG interconversions. Droplets were counted in at least 3 random fields, approximately 20 cells per field; mean ± SE shown. (*$p < 0.05$, *** $p < 0.0001$). (C), Comparison of DAG and PA levels of the WT and *dgk1Δ*, showing an increase in DAG and decrease in PA in the mutant. Error bars are SE. (D) Histogram showing the percentage of cells with "pearls on a string" lipid droplet phenotype, mean ± SE (** $p < 0.001$)

unable to synthesize TAG (*dga1Δ lro1Δ*). In this mutant, the knockout of *DGK1* resulted in the formation of more droplets and an enhancement of the "pearls on a string" phenotype when compared to *dga1Δ lro1Δ* (Figure 10 A and D). These data indicate that DAG facilitates lipid droplet formation independent of its role in the synthesis if TAG.

The Pah1p phosphatase resides close to lipid droplets

Diacylglycerol should be produced at the site of droplet formation for it to be active otherwise it would rapidly diffuse laterally in the membrane. As mentioned earlier, Pah1p is mostly cytosolic but, becomes membrane-localized once dephosphorylated by the membrane associated protein phosphatase complex, Nem1p/ Spo7p (Choi et al., 2011; Karanasios et al., 2010; Santos-Rosa et al., 2005). Fluorescence microscopy confirmed that chromosomally labeled Pah1p was cytosolic because no clear localization of Pah1p-GFP could be observed (Figure 11 B). On the other hand, the Nem1p/ Spo7p complex was uniquely localized to a single punctum per cell (Figure 11 A). Furthermore, the Nem1p-mCherry punctum was observed on the ER and in close proximity to BODIPY-stained droplets (Figure 12 A). By scoring the proximity of Nem1p-mCherry to droplets in three dimensions, 77 % of them appeared to be in contact with droplets, whereas only 13 % could clearly be resolved from droplets (Figure 12 B). The proximity to droplets was clearly visualized in a computer-aided

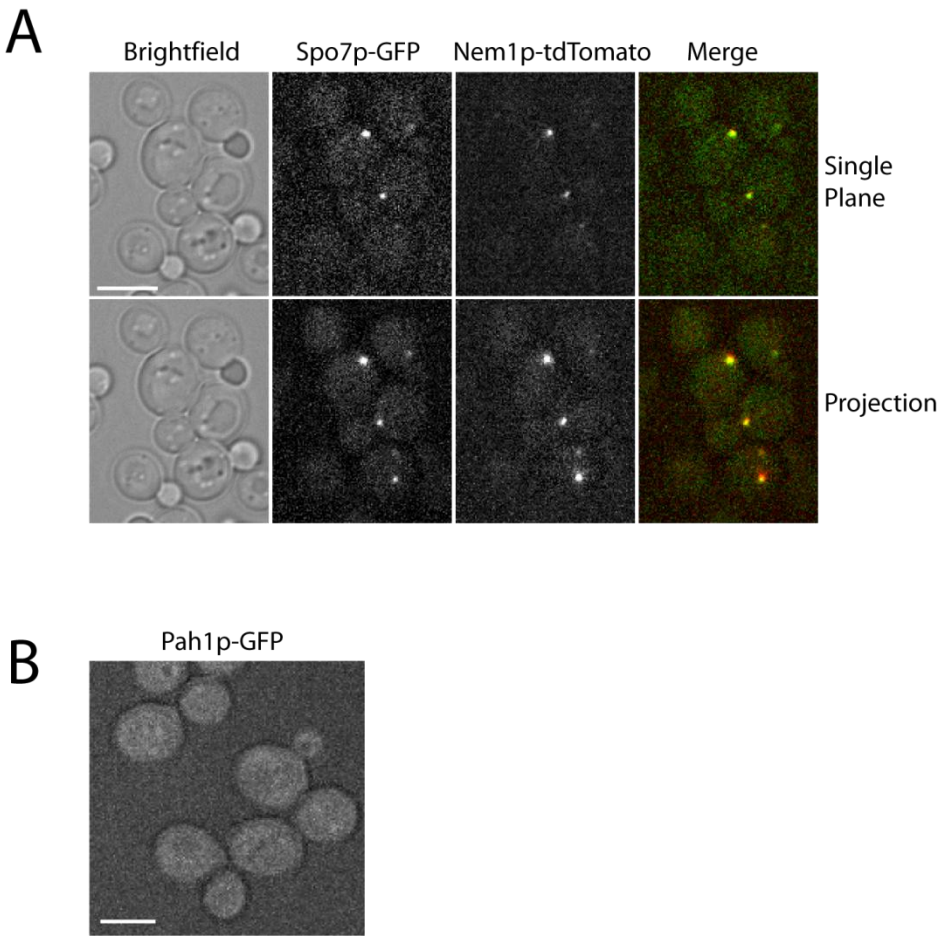

Figure 11. Pah1p activators Nem1p and Spo7p colocalize. (A) Localization of chromosomally expressed GFP-tagged Spo7p and tdTomato tagged Nem1p. Yeast strains were cultured in SD. Single Z-section (top) and projection image (bottom) the same field is shown. (B) Localization of chromosomally expressed Pah1p-GFP. Merged image with brightfield is shown to outline cell position. Strains cultured in SD. Scale bar, 5 μm.

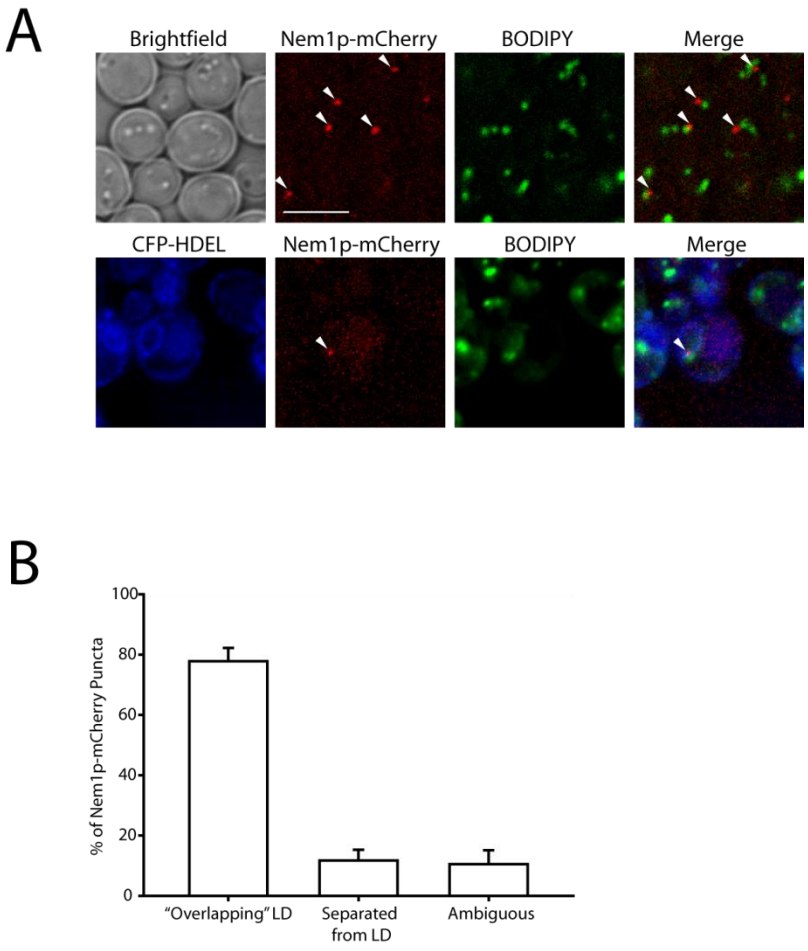

Figure 2. Nem1p localizes next to lipid droplets on the ER. (A) Nem1p-mCherry was chromosomally expressed at the *NEM1* locus. Lipid droplets were stained with BODIPY and cells were expressing CFP-HDEL (bottom row only). Arrowhead shows juxtaposition of BODIPY (LD) and Nem1p-mCherry (top row) as well as CFP-HDEL (ER), BODIPY, and Nem1p-mCherry. Scale bar, 5 μm. (B) Histogram showing juxtaposition of Nem1p-mCherry puncta with lipid droplets. Nem1p-mCherry puncta were counted from seven separate groups of cells and scored for their observed association with lipid droplets. Mean ± SE was calculated across all seven groups.

3D volume rendering of a Z-stacked field of cells in which 10 out of 12 Nem1p-mCherry puncta within the field were within 0.65 μm of a droplet (Figure 13).

Nem1p-mCherry colocalization with droplets was also observed by fluorescence microscopy in membranes derived from post-nuclear supernatants of cells expressing Nem1p-mCherry in the genome (Figure 14). Isolated membranes from cells grown in glucose medium contained droplets that remained attached to the ER and associated with Nem1p puncta. In contrast, when membranes containing CFP-HDEL were analyzed, no colocalization with lipid droplets was observed. This data suggests that DAG is produced by Pah1p at the site of droplet formation where it plays an important role in lipid droplet biogenesis.

If Nem1p marks the site where nascent droplets are formed, it should colocalize with the first droplet in a system in which droplet formation can be regulated. To test this hypothesis, quad mutants (which are unable to make droplets) chromosomally expressing Nem1p-tdTomato were transformed with plasmid constructs containing the *DGA1* open reading frame under the control of a galactose-inducible promoter. With this system TAG containing droplets will only be formed when the cells are cultured in media containing galactose, more importantly, droplet formation can be monitored along with the localization of the Nem1p punctum.

With the droplet-induction system, lipid droplets assembled asynchronously in only about 50 % of cells, and because of this, data was

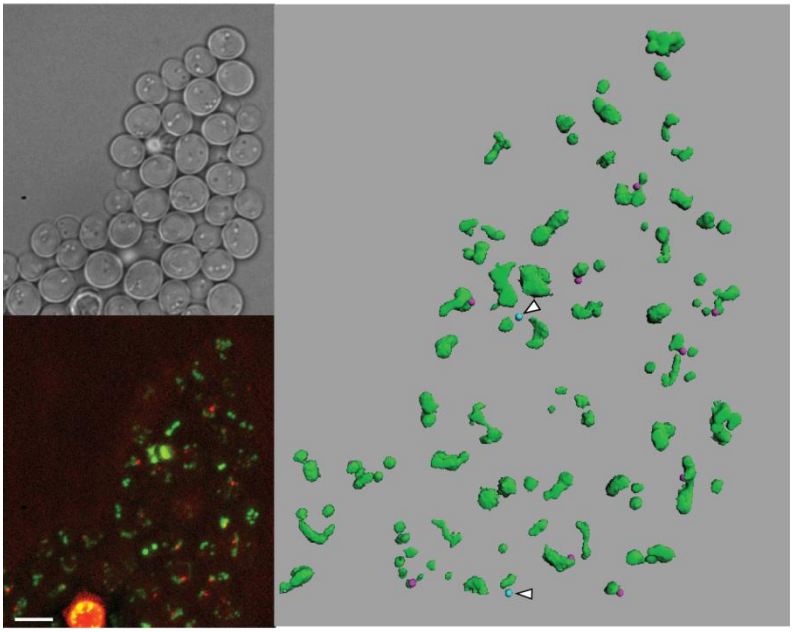

Figure 13. Nem1p localizes next to lipid droplets. Nem1p-mCherry was chromosomally expressed at the *NEM1* locus. Lipid droplets were stained with BODIPY. Top left: brightfield image. Bottom left: projection image of BODIPY stained cells showing Nem1p-mCherry localization. Scale bars, 5 µm. Right: 3-dimensional reconstruction of the same field of cells. Green, droplets; pink (approximately 10 examples in this field of view), Nem1p within 0.65 µm of a droplet surface; blue (2 examples with arrowheads), Nem1p-mCherry beyond 0.65 µm of a droplet.

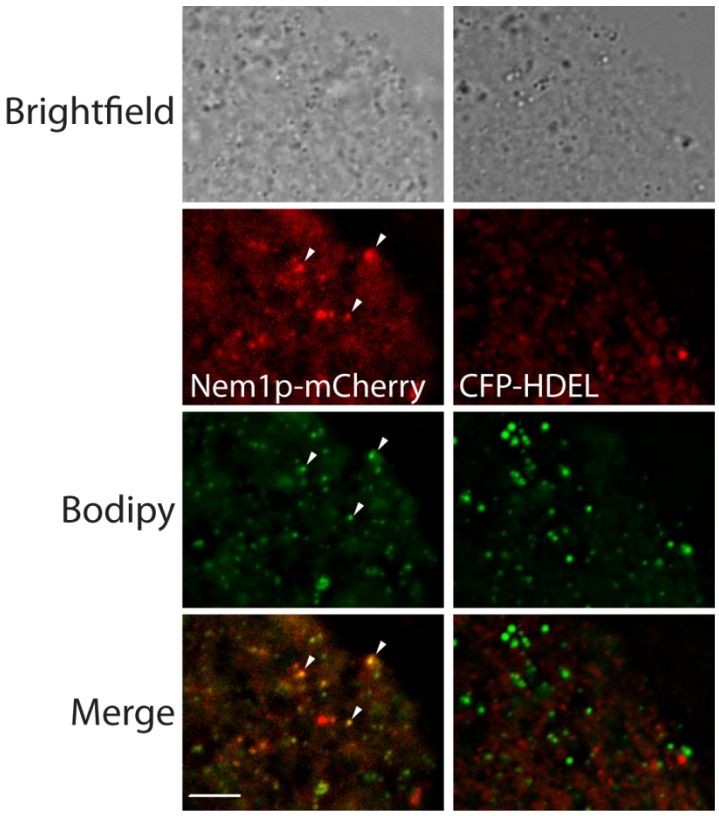

Figure 3. Colocalization of Nem1p-mCherry and droplets in isolated membranes. Membranes derived from post-nuclear supernatant of yeast strains containing chromosomally expressed Nem1p-mCherry (left) or plasmid expressed PGK CFP-HDEL (right) were stained with BODIPY.

obtained only from cells that had both Nem1p-tdTomato signal as well as lipid droplets. I observed that Nem1p localized to a single puncta (similar to the localization observed in wild-type) as well as a diffuse pattern that encompassed a small portion of the cell (Figures 15-18). During the induction, the single punctum appeared to precede the formation of the diffuse pattern (Figure 15 and 16), although, in some instances the diffuse pattern was present at the earliest time points observed (Figure 17).

From data obtained only about 17 % of cells had a BODIPY-stained lipid droplet that originated from the Nem1p-tdTomato punctum (Figure 15). Approximately 44 % of cells had droplets that originated within regions that contained the diffuse Nem1p-tdTomato signal (Figures 16 and 17), while 39 % of cells had droplets that formed away from any Nem1p-tdTomato signal (Figure 18). This data suggests that Pah1p may regulate the biogenesis of some but not all TAG-containing lipid droplets.

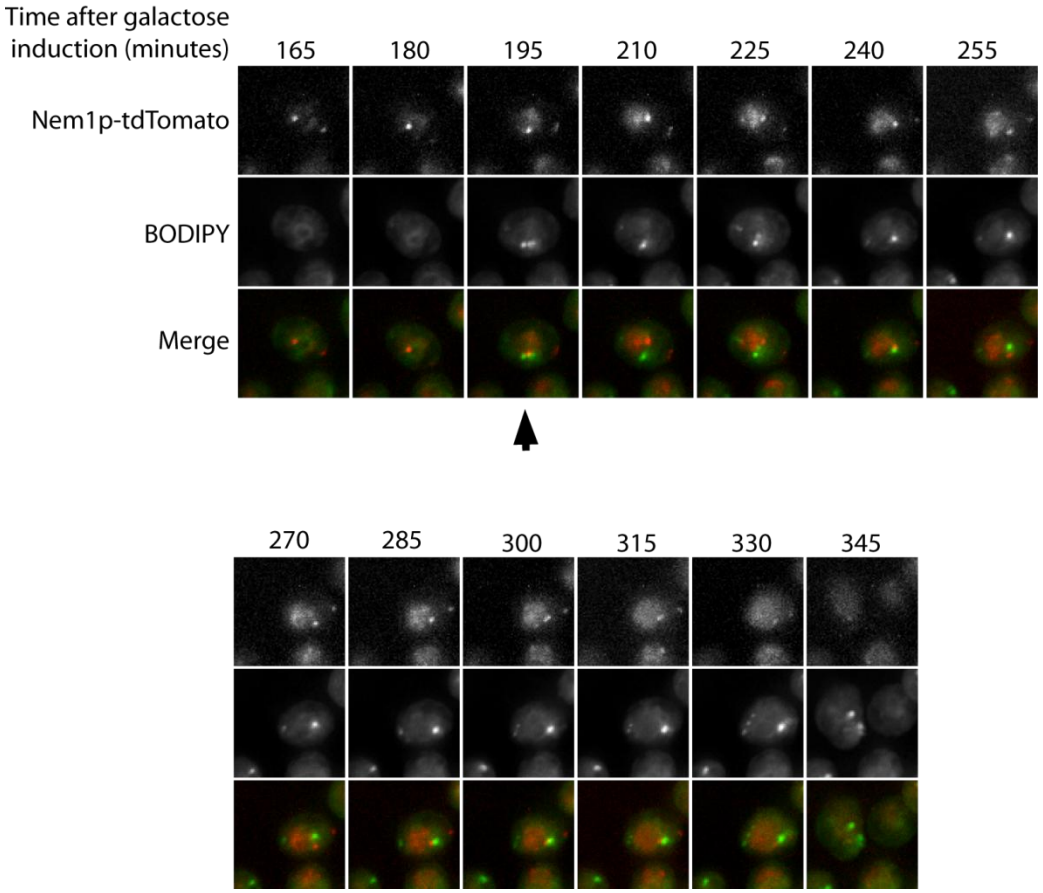

Figure 4. Time-lapse fluorescence microscopy showing new lipid droplet originating from Nem1p puncta. Lipid droplets are BODIPY stained (green) and cells are chromosomally expressing tdTomato tagged Nem1p (red). Projection images are shown. Bottom arrow indicates a time point where a new lipid droplet assembles at the Nem1p-tdTomato punctum.

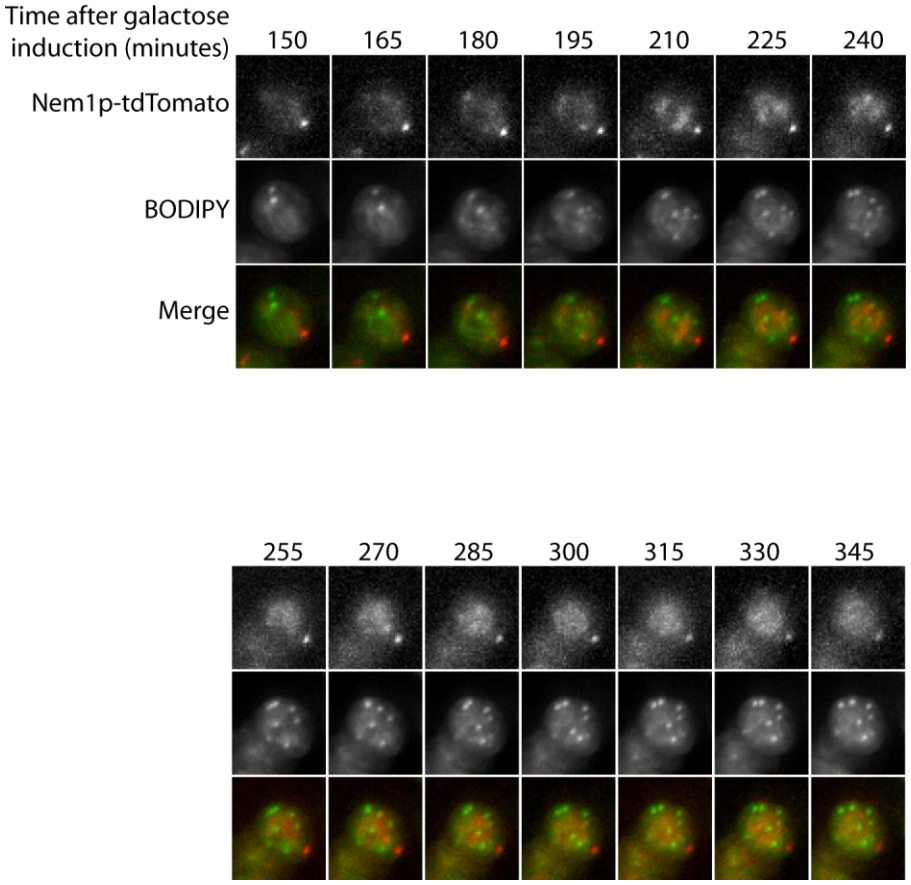

Figure 5. Time-lapse fluorescence microscopy showing new lipid droplets originating from dispersed Nem1p. Lipid droplets are BODIPY stained (green) and cells are chromosomally expressing tdTomato tagged Nem1p (red). Projection images are shown.

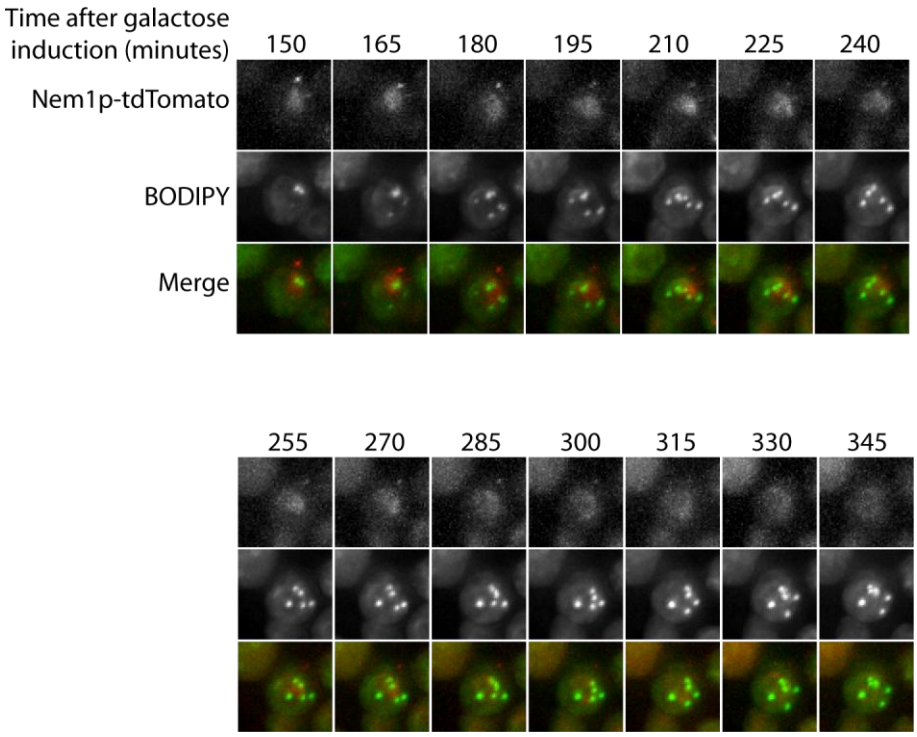

Figure 6. Time-lapse fluorescence microscopy showing dispersed Nem1p signal at early time points. Lipid droplets are BODIPY stained (green) and cells are chromosomally expressing tdTomato tagged Nem1p (red). Projection images are shown.

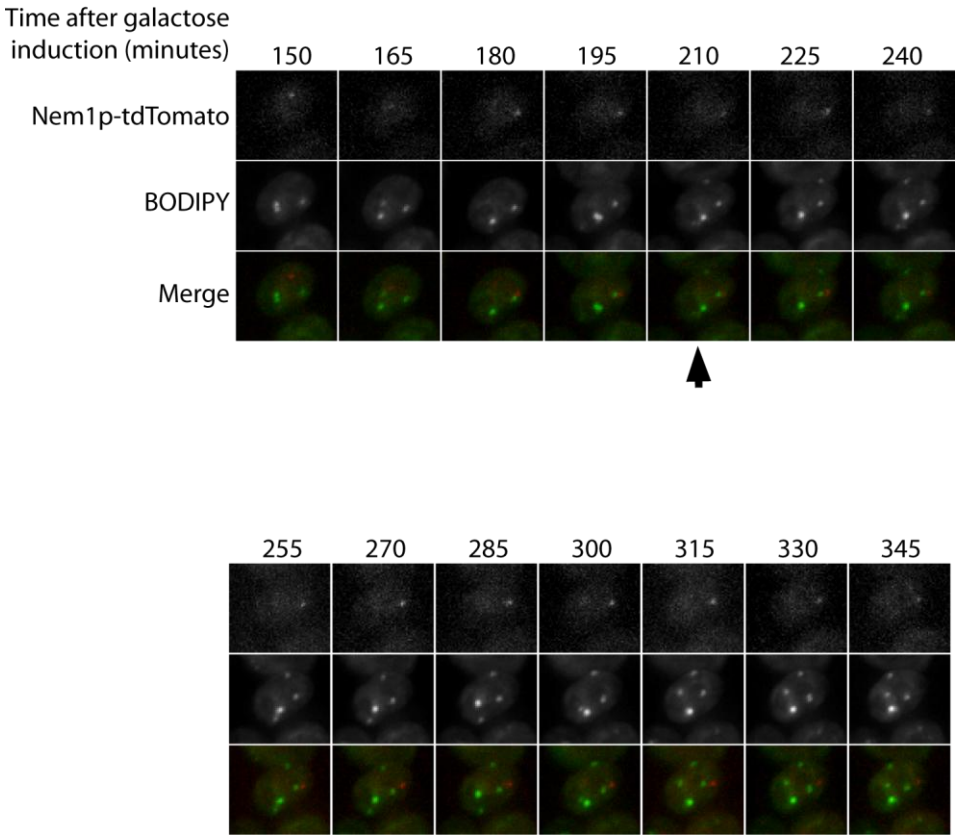

Figure 7.Time-lapse fluorescence microscopy showing new lipid droplets originating away from Nem1p puncta. Lipid droplets are BODIPY stained (green) and cells are chromosomally expressing tdTomato tagged Nem1p. Projection images are shown. Bottom arrow indicates a time point where a new lipid droplet assembles away from the Nem1p-tdTomato punctum

Discussion

It was previously reported that mammalian lipid droplet coat proteins such as Perilipin 3 are recruited to DAG enriched ER membranes (Skinner et al., 2009). Here I have presented several lines of evidence to suggest that localized DAG synthesis may facilitate lipid droplet formation in *Saccharomyces cerevisiae*. First, the absence of Pah1p PAP activity results in reduced lipid droplet number. Second, a knockout of Dgk1p which negatively regulates DAG synthesis results in an increase in lipid droplet formation even in the combined absence of TAG synthesis. Third, the protein phosphatase and Pah1p activator Nem1p, is localized next to droplets. Last of all, some nascent droplets originate from regions where Nem1p is localized. However, It is important to note that the in vivo approach used in the experiments above cannot rule out the potential effects of other lipids, the concentration of which are altered in the *pah1Δ* strain (Han et al., 2006).

How diacylglycerol may facilitate lipid droplet formation remains unknown. The effect of DAG in perturbing phospholipid bilayers, promoting high curvature of leaflets, and conversion to hexagonal phase structures is well known (Goñi and Alonso, 1999). DAG clearly promotes budding and fission of vesicles from membranes such as the Golgi complex (Asp et al., 2009; Roth, 1999). Although DAG can bend a membrane even more than PA because of its smaller head group, it is unstable in the bilayer and can rapidly flip-flop between leaflets

of the bilayer (Pagano and Longmuir, 1985), leading to membrane instability that may promote the formation of the droplet bud. It is also possible that DAG plays an indirect role to facilitate formation of a droplet. For example, DAG may recruit other molecules important for trafficking, such as ARF GTPase-activating protein (Antonny et al., 1997), or in mammalian cells, structural lipid droplet proteins such as Perilipin-3 (Skinner et al., 2009).

It is interesting that disruption of *DGK1* results in increased lipid droplet formation independent of TAG synthesis. The fact that whole cell DAG levels are not significantly altered in the absence of Dgk1p may suggest the existence of microdomains of the ER where high DAG concentrations can facilitate lipid droplet formation. Florescence microscopy of GFP tagged Dgk1p indicated that the protein is evenly distributed on the ER membrane (Han et al., 2008a). I envision that the role of Dgk1p as a DAG kinase also serves to negatively regulate lipid droplet formation in areas away from the DAG rich microdomains. When DAG concentration is uncontrolled in *dgk1Δ*, spontaneous droplet formation may occur, leading to the pearls on a string droplet phenotype (Figure 10 A and D)

Uncontrolled DAG synthesis can also bypass the Pah1p requirement for efficient lipid droplet formation. This is observed in the *pah1Δ dgk1Δ* mutant whose lipid droplet number far exceeds that of *pah1Δ* (Figure 10 B). The mutant (*pah1Δ dgk1Δ*) also contains more TAG than *pah1Δ* cells but not as much as WT or *dgk1Δ* alone (Figure 10 B. inset). The question still remains to be answered on

what protein synthesizes the DAG to facilitate droplet formation or make TAG in this mutant. Dpp1p is understood to not be involved in denovo synthesis of phospholipids or TAG (Han et al., 2006). However, the protein has broad substrate specificity for its PAP activity and it regulates the cellular levels of PA and DAG pyrophosphate on vacuolar membranes of zinc depleted cells (Han et al., 2004). When Pah1p is absent, perhaps some of the lipid droplets in the *pah1Δ dgk1Δ* originate from vacuolar membranes facilitated by Dpp1p PAP activity. If this is the case, transmission EM images of this mutant would be expected to show increased LD interaction with vacuoles.

About 30 % of the magnesium-dependent PAP activity in isolated *Saccharomyces cerevisiae* membranes is originates from an unknown phosphatase (Han et al., 2006). Triglyceride levels are slightly increased and lipid droplet number is significantly increased in the *pah1Δ dgk1Δ* mutant compared to *pah1Δ* alone. If these changes are attributed to the unknown enzyme, the *pah1Δ dgk1Δ* mutant may be the ideal candidate to discover the identity of the unknown phosphatase. Preliminary results to determine if droplets in the *pah1Δ dgk1Δ* mutant are facilitated by magnesium-dependent PAP activity, might be obtained by growing the mutant in magnesium-deficient media to see if LD number and TAG levels remain the same as mutants grown in media containing magnesium.

The proximity of Nem1p to nascent droplets suggests that Pah1p docks at or within the vicinity of the Nem1p/ Spo7p complex, where it provides DAG (and

later TAG) to facilitate droplet formation. The galactose induction experiments demonstrate that about 17 % of droplets originate from Nem1p-tdTomato puncta while 44 % originate from areas where Nem1p-tdTomato localization is diffuse. With the current data, I am unable to determine the specific organelle within the cell in which the dispersed Nem1p-tdTomato signal resides. Therefore, fluorescently tagged organelle markers will have to be included in further experiments. Nevertheless, it is possible that the dispersed Nem1p may be nuclear, consistent with the localization observed for its mammalian homologue (Dullard), and the association of Pah1p with promoters of phospholipid biosynthetic enzymes (Kim et al., 2007; Santos-Rosa et al., 2005).

Due to the fact that Nem1p has a transmembrane helix and ER localization signal, I favor the possibility that diffuse Nem1p may still be ER localized, but fewer copies of the protein away from its expected punctuate localization may not be easily detected by basic epi-fluorescence microscopy techniques used in the experiment. Nem1p may be redistributed in response to droplet formation from its single location to other regions along the ER. This redistribution may allow Nem1p to activate cytosolic Pah1p at other regions of the ER allowing for a more efficient means of droplet biogenesis at multiple locations on the ER rather than only at the single punctum alone. The 15-minute intervals in which the data was obtained may not be sufficient to accurately observe the precise dynamics for

droplet formation. Similar experiments utilizing spinning disc confocal microscopy may provide more detailed results.

Although the droplet induction system allows us to observe early droplet assembly, droplet formation is asynchronous making it difficult to compare data from multiple cells within a given timepoint. The diffuse Nem1p pattern at the early timepoints may be present because of this asynchronous nature. They may represent cells in which Pah1p dependent droplet assembly has already been initiated before the cells are observed by microscopy (see materials and methods).

One major caveat with the use of fluorescent microscopy to monitor droplet biogenesis is that it limits the data obtained to signals detected from neutral lipid dyes. A nascent droplet may be so small that even if it was assembled at the Nem1p punctum, it may not be detected by the neutral lipid dye until it has migrated away from its region of origin. Immunogold electron microscopy (labeling Nem1p) performed at different time-points during droplet induction would verify the origins of a nascent droplet.

Nevertheless, the time course data for droplet formation demonstrated that 61 % of cells had droplets that originated from regions with the Nem1p-tdTomato signal. This data along with the fact that *pah1Δ* mutants still have 37 % of wild-type droplets strongly suggests that Pah1p cannot be the only means for droplet formation in *Saccharomyces cerevisiae*. It is also important to note that the time-course experiment focuses exclusively on TAG containing droplets generated by

Dga1p, but as mentioned earlier, a single droplet could contain TAG and/ or StE and the contributions of the other neutral lipid synthesizing enzymes to the biogenesis of a mature droplet is clearly excluded from the experiment. Similar experiments inducing steryl acyltransferase expression would be required to determine if Pah1p is also required for the biogenesis of StE containing droplets and would be consistent with data showing that *pah1Δ* membranes contain more StE than wild-type (Figure 6).

CHAPTER 5

Fld1p AND LIPID DROPLET BIOGENESIS

Introduction

Congenital generalized lipodystrophy (CGL) is a rare autosomal recessive disorder characterized by loss of adipose tissue, fatty liver, insulin resistance and hypertriglyceridemia (Agarwal and Garg, 2006). Genome-wide linkage analysis identified the most severe form of CGL to be caused by mutations to the Berardinelli-Seip congenital lipodystrophy 2 (BSCL2) gene which encodes seipin (Agarwal and Garg, 2004; Magre et al., 2001). In spite of this, the molecular function of seipin remains unknown. Studies from the Goodman lab and others have shown that seipin regulates adipogenesis in mammals and is required to maintain lipid droplet morphology in both mammals and *Saccharomyces cerevisiae* (Chen et al., 2009; Fei et al., 2008; Fei et al., 2011; Magre et al., 2001; Szymanski et al., 2007). Insights into the role of yeast seipin (Fld1p) in lipid droplet formation will be the main focus of this chapter.

Fld1p was the first protein observed to localize specifically at junctions between the lipid droplets and ER membranes in yeast, suggestive of a functional role in lipid droplet biogenesis and/ or maintenance (Szymanski et al., 2007). Although the protein resides on the ER through two transmembrane domains, no

recognizable functional domain or motif has been identified (Agarwal and Garg, 2004). A knockout or mutations to seipin result in the formation of lipid droplets that are small and clustered or abnormally large in size (Fei et al., 2008; Szymanski et al., 2007). These alterations in lipid droplet morphology were also evident in seipin deficient fibroblasts suggestive of a role in lipid droplet formation conserved from yeast to mammals.

Experiments in this chapter are designed to better understand the association of Fld1p with lipid droplets as well as trafficking of the protein during LD biogenesis in *Saccharomyces cerevisiae*. I show that lipid droplets are always associated with Fld1p regardless of changes to cellular droplet number or size. However, a reduction in droplet number or increases in lipid droplet size resulted in localization of some Fld1p molecules away from lipid droplets. Finally, I demonstrate that lipid droplets originate from Fld1p enriched regions of the ER.

Materials and Methods

Strains and Culture Conditions

All yeast strains and plasmids used in this chapter are listed in Table 4. Cells were cultured as described in Chapter 2

Fluorescence Microscopy

Images were acquired as described in Chapter 2.

To monitor droplet biogenesis (Figure 22), aliquots from cultures grown in minimal galactose media were obtained at the indicated time points, stained with BODIPY and observed for Fld1p association with lipid droplets.

SDS-Polyacrylamide Gel Electrophoresis and Immunoblotting

Standard 10 % Laemmli gels were used (Laemmli, 1970). Immunoblotting was performed with an ECL kit (Amersham). The monoclonal anti-myc antibody was purchaced from the National Cell Culture Center (Minneapolis, MN), and used at 1:1000 dilution. Glucose-6-phosphate dehydrogenase (Zwf1p) antibody (Sigma-Aldrich) was used at 1:10000 dilution.

Table 4. Plasmids and Yeast Strains Used in This Chapter

Plasmid	**Relevant characteristics**	**Source or reference**
pRS314	Ecoli/ yeast vector with TRP1	(Sikorski and Hieter, 1989)
pRS314-PGK	pRS314 containing PGK1 promoter and terminator	This study
pRS314-PGK-CFP-HDEL	pRS314-PGK containing CFP-HDEL inserted into Xho1/ SacII sites	This study
pRS314-GAL10	pRS314 containing GAL10 promoter and PGK1 terminator	This study
DB001	pRS314-GAL10 containing DGA1 inserted into BamHI and HindIII sites	This study
Strain	**Genotype** (all *Saccharomyces cerevisiae*)	
BY4742	Matα his3Δ1 leu2Δ0 lys2Δ0 ura3Δ0	Open Biosystems
SCY328	MATa ade2-1 his3-11,15 leu2-3,112,trp1-1ura3-1 can1	(Valachovic et al., 2006)
SCY1998	*dga1Δ::URA3, lro1Δ::LEU2*	Gift from S. Sturley
SCY1703	*are1Δ::HIS3, are2Δ::LEU2*	Gift from S. Sturley
SCY2021	*dga1Δ::URA3, lro1Δ::URA3, are1Δ::LEU2, are2Δ::HIS3*	Gift from S. Sturley
OAS005	SCY328 (*dgk1Δ::HIS3*)	This study
OAS007	SCY1998 (*dgk1Δ::HIS3*)	This study
SKS001	SCY328 strain with tdTomato at the c-terminus of the *FLD1* ORF	This study
SKS002	SCY1998 strain with tdTomato at the c-terminus of the *FLD1* ORF	This study
SKS003	SCY1703 strain with tdTomato at the c-terminus of the *FLD1* ORF	This study
SKS004	SCY2021 strain with tdTomato at the c-terminus of the *FLD1* ORF	This study
OAS009	SKS001 (*dgk1Δ::HIS3*)	This study
OAS010	SKS002 (*dgk1Δ::HIS3*)	This study

Results

Conditions that alter Fld1p localization

As mentioned earlier, Fld1p localized to the junction between lipid droplets and the ER suggestive of a role in droplet biogenesis or maintenance. The main constituents of the LD core are triglycerides and steryl esters, although the mechanism that regulates how these individual neutral lipids are shuttled from the ER in to lipid droplets remains unknown. I demonstrated previously that lipid droplets are fewer in the absence of the DAG acyltransferases (which generate TAG. Figure 7), and I wondered if this reduction in lipid droplet number would have an effect on the association of Fld1p with the remaining lipid droplets. To answer this, *FLD1* was chromosomally tagged with tdTomato in wild-type, as well as cells that lacked the DAG acyltransferases (*DGA1* and *LRO1*) or the steryl acyltransferases (*ARE1* and *ARE2*). In wild-type cells, Fld1p-tdTomato always associated with a lipid droplet (Figure 19 A). However, Fld1p-tdTomato did not associate exclusively with lipid droplets in the *are1Δ are2Δ* and *dga1Δ lro1Δ* mutant strains, since some of the Fld1-tdTomato signal was observed at the cortical ER away from lipid droplets (Figure 19 A). We defined Fld1-tdTomato patches that did not interact with lipid droplets as ‘orphan seipin’. Interestingly, orphan seipin was more prominent in *dga1Δ lro1Δ* compared to *are1Δ are2Δ*, and it is worth noting that the latter had fewer lipid droplets. When cells are unable to make lipid droplets (in the quad mutant which lacks all four acyltransferases),

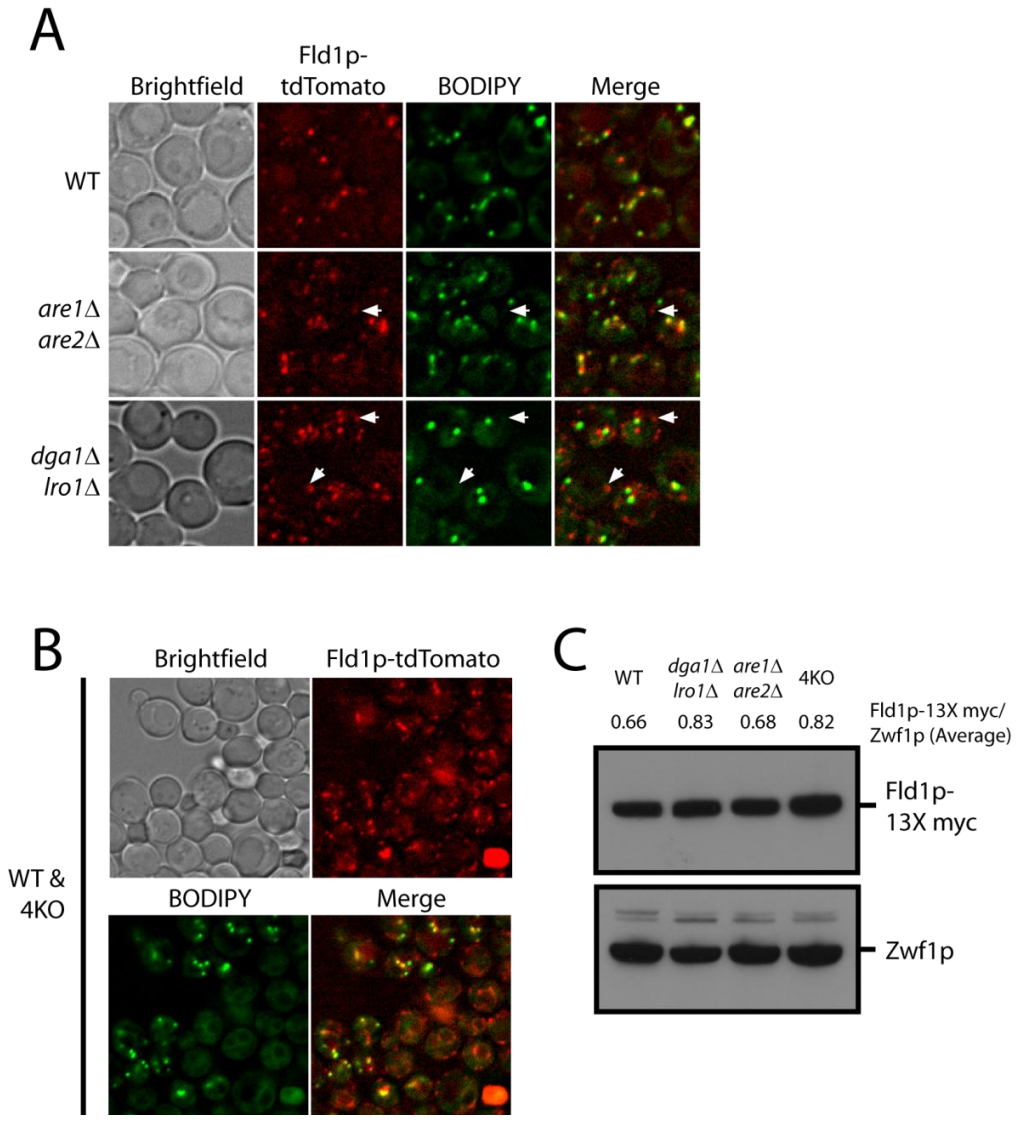

Figure 8. Fld1p always interacts with lipid droplets but will form orphans when droplets are scarce or unavailable. (A) The indicated yeast strains were chromosomally expressing Fld1p-tdTomato (red) and stained with BODIPY (green); arrows identify orphan seipin. (B) One-to-one mix of wildtype and 4KO (*dga1Δ lro1Δ are1Δ are2Δ)* chromosomally expressing Fld1p-tdTomato. Strains can be distinguished by the presence and absence of BODIPY stained droplets. Note that Fld1p still retains its patchy localization along the ER of 4KO. (C) Western blot showing expression level of Fld1p-13x myc in the strains listed above. Values shown above the blot are corrected to that of Zwf1p, and represent an average of two independent experiments.

Fld1p-tdTomato signal appeared as patches evenly distributed on the cortical and perinuclear ER (Figure 19 B). These patches were not as intense as Fld1p patches that associated with lipid droplets (compare Fld1p localization in cells with droplets to those without in Figure 19 B). In spite of the changes in Fld1p localization observed with alterations to lipid droplet number (or neutral lipid content), there was only a slight increase in Fld1p expression when orphan seipin was present, but, no change in molecular weight to suggest any manner of posttranslational modification (Figure 19 C). These data confirms that Fld1p intimately associates with individual lipid droplets on the ER and suggests that the presence of lipid droplets somehow organizes Fld1p on ER membranes.

When lipid droplet number in the *dga1Δ lro1Δ* mutant is increased by knocking out *DGK1*, all visible droplets were still associated with Fld1p. However, the increase in lipid droplet number did not eliminate orphan seipin (Figure 20).

Because alterations to the localization of Fld1p were observed when lipid droplet numbers are reduced, I hypothesized that increasing lipid droplet size would promote Fld1p interaction with lipid droplets. On the contrary, when wild-type cells are cultured in oleic acid media (which significantly increases lipid droplet size), Fld1p-tdTomato was observed as ‘orphan seipin’ as well as distinct puncta on the ER associating with droplets. All observable droplets had an

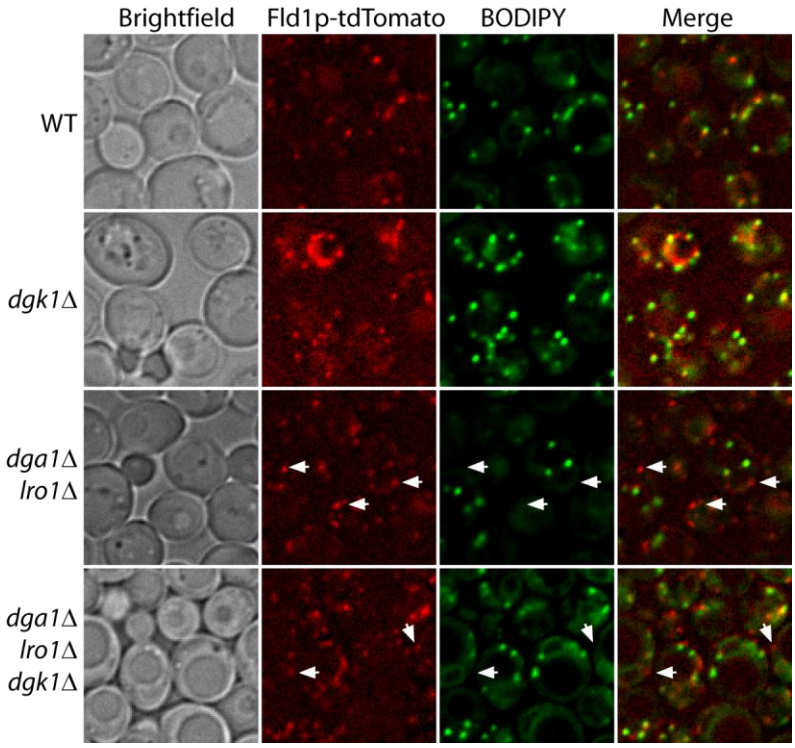

Figure 9. Increasing lipid droplet number in *dga1Δ lro1Δ* does not reduce the occurrence of orphan seipin. The indicated yeast strains were chromosomally expressing Fld1p-tdTomato (red) and stained with BODIPY (green); arrows identify orphan seipin.

Fld1-tdTomato signal adjacent to it, but not all Fld1-tdTomato signals were present on droplets (Figure 21 A). Yet again, a condition resulting in the presence of 'orphan seipin' showed a slight increase to Fld1p expression, but no change in molecular weight to suggest posttranslational modification (Figure 21 B).

Fld1 and lipid droplet biogenesis

Lipid droplets always associate with Fld1p, and in their absence, Fld1p is dispersed on the ER, especially on the cell cortex. It is known that lipid droplet morphology is significantly altered in the absence of Fld1p (Fei et al., 2008; Szymanski et al., 2007), but how Fld1 regulates this process is unclear. Droplet morphology in *fld1Δ* could be altered at the stage of droplet biogenesis in which the droplets emanate abnormally from the ER. An example of this was seen by transmission electron microscopy of the *fld1Δ* mutant in which the ER was observed to wrap around tiny droplet clusters (Szymanski et al., 2007). These data were supported by lipid analysis of droplet and microsomal fractions in which the *fld1Δ* mutant ER microsomes contained more neutral lipid than wild-type (Figure 22 A). The data indicate that droplets from *fld1Δ* have a stronger association with the ER membrane than WT which cannot be completely separated by centrifugation, or that the ER itself contains more neutral lipid.

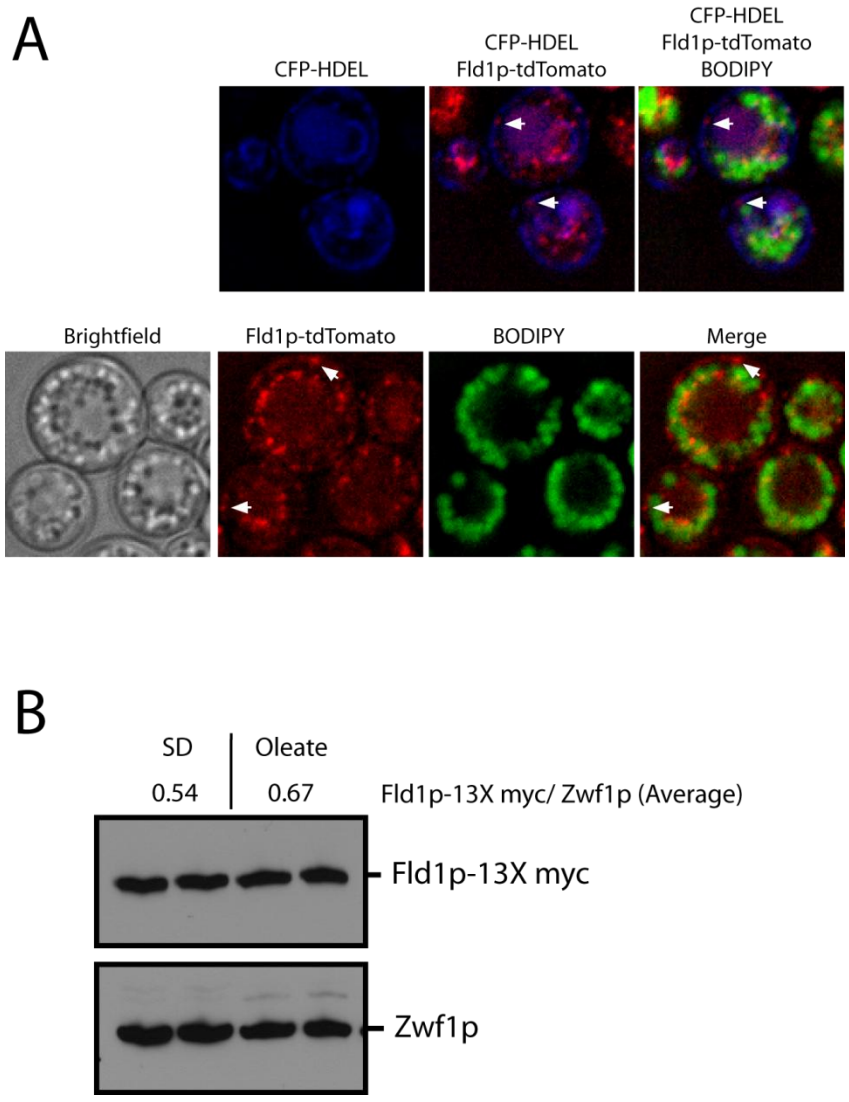

Figure 10. Orphan seipin is present when cells are cultured in oleic acid-containing medium. Fld1p-tdTomato was chromosomally expressed at the *FLD1* locus in wild-type yeast cells cultured overnight in oleic acid-containing medium. Lipid droplets were stained with BODIPY and cells were expressing CFP-HDEL (top row only). Arrows identify orphan seipin. (B) Western blot showing expression levels of Fld1p-13x myc in wild-type cultured in SD and oleic acid-containing medium. Values shown above the blot are corrected to that of Zwf1p, and represent an average of two independent experiments.

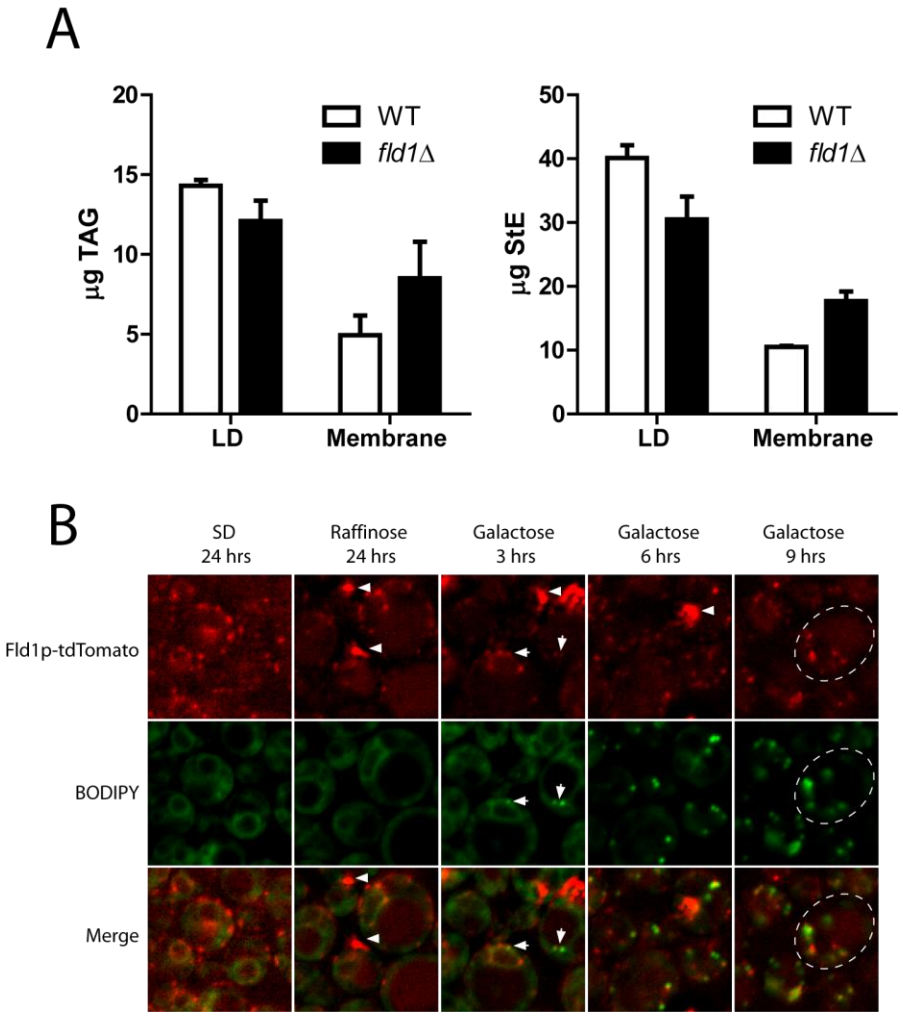

Figure 11. New droplets originate from regions containing Fld1p. (A) Lipid droplet and membrane levels of TAG (left) and StE (right) in the indicated strains. Post nuclear extracts from spheroplasts (grown in SD) were fractionated by centrifugation. An identical percentage of floating droplets and membrane pellets, normalized to total protein in extracts, were subjected to TLC. Error bars indicate the range of values from two independent experiments. (B) Fld1p-tdTomato was chromosomally expressed at the *FLD1* locus in a 4KO mutant. Lipid droplets were stained with BODIPY and cells were expressing Dga1p under the control of a galactose inducible promoter. Images were acquired from aliquots obtained during growth in the culture medium, and at timepoints listed above. Arrows identify Fld1p interacting with lipid droplets. Arrow heads identify seipinosomes. Dashed white lines in the last column outline the region occupied by a cell to emphasize perinuclear localization of Fld1p at the indicated timepoint

If the lipid droplet-ER connection is abnormal in *fld1Δ* perhaps Fld1p organizes ER membranes in preparation for lipid droplet assembly. For Fld1p to function in this manner, it would have to reside where a lipid droplet originates. I tested this idea by inducing droplet formation in quad mutants that chromosomally express Fld1p-tdTomato and indeed, nascent droplets originated from ER regions with an Fld1p-tdTomato signal (Figure 22 B). Furthermore, with increased growth in galactose, Fld1p appeared to localize predominantly on the perinuclear ER rather than the cortical ER as observed when lipid droplets are absent (Compare Fld1-tdTomato localization at 9 hrs galactose to raffinose or glucose cultures in Figure 22 B).

Considering that growth in oleic acid containing media alters the localization of Fld1p, an interesting phenomenon was observed in which Fld1p clustered towards the cortical regions of the quad mutant cells that were cultured in raffinose media. We called these Fld1p clusters seipinosomes and they were absent in glucose grown cultures and disappeared when raffinose grown cells were transferred to galactose or glucose medium. The disappearance of seipinosomes in galactose media appeared to be independent of lipid droplet formation, because it was observed in galactose-grown quad mutants. The reason for seipinosome formation is unknown at present; however, it is another example of an alteration to Fld1p localization in response of a change in growth medium.

Discussion

The fact that Fld1p retains its patchy localization on the ER in the absence of lipid droplets coupled with the observation that new droplets originate from Fld1p patches (Figure 22 B) indicates that Fld1p may prime these ER sites for lipid droplet assembly. This idea would be consistent with abnormal lipid droplet morphology observed in *fld1Δ* mutants (Fei et al., 2008; Szymanski et al., 2007).

Orphan seipin was absent in *dgk1Δ* cells which have a higher number of lipid droplets than wild-type. Furthermore, its appearance was not increased in DAG acyltransferase mutants which have increased droplet number due to the absence *DGK1* (compare orphan seipin presence in *dga1Δ lro1Δ* to *dgk1Δ dga1Δ lro1Δ*). I conclude from these data that an increase in lipid droplet number alone is not sufficient to induce the assembly of orphan seipin. However, orphan seipin was present in wild-type cells cultured in oleic acid-containing medium. Cells cultured in media containing oleic acid would have increased free fatty acid load, and neutral lipid synthesis will have to be amplified for energy storage, and to prevent free fatty acid induced lipotoxicity. The increase in orphan seipin observed in oleic acid-grown cultures may therefore be a response to an increased requirement for lipid droplets due to elevated neutral lipid synthesis. This finding supports the hypothesis that Fld1p primes ER sites for droplet assembly. A model describing how Fld1p may function in this manner is discussed in Chapter 6.

The conclusion that lipid droplets originate from Fld1p patches is based on static images obtained at different time points. Ideally, time-lapse fluorescence would be required to verify this observation. Nevertheless, as mentioned before, the experiment is still restricted by the sensitivity of the microscope's ability to detect BODIPY-stained neutral lipids. Again, electron microscopy coupled with immunogold labeling of Fld1p would be required to verify this event. If newly formed droplets originate elsewhere on the ER and are then transported to Fld1p, it would suggest that Fld1p is involved in lipid droplet maintenance rather than biogenesis.

Synthetic phospholipid bilayers can contain a small amount of neutral lipid while still remaining stable (Hamilton, 1989) and, I have shown that isolated yeast membranes contain small amounts of neutral lipid as well (Figure 6 and 22 B). Others have suggested that Fld1p could function to regulate the metabolism of phospholipids and glycerolipids, because *fld1Δ* cells have phospholipids with shorter and more saturated fatty-acyl chains (Fei et al., 2008). It is possible that the increase in saturated fatty-acyl chains of phospholipids reduces membrane fluidity thereby inhibiting the budding of droplets from the ER. This would explain the increase in membrane neutral lipids observed in *fld1Δ*.

CHAPTER 6

GENERAL DISCUSSION AND FUTURE DIRECTIONS

Working model

I have provided evidence in this dissertation to suggest that the phosphatidic acid hydrolase (Pah1p) is involved in the biogenesis of lipid droplets through the synthesis of diacylglycerol. A working model highlighting the involvement of Pah1p is shown in Figure 23. Several copies of the Nem1p/ Spo7p phosphatase complex reside in a single location on the ER membrane. Neutral lipid synthesis may induce translocation of single copies of the phosphatase complex to other regions of the ER or expression of new phosphatases away from the complex cluster. Cytosolic Pah1p is dephosphorylated by (either clustered or dispersed) Nem1p/ Spo7p phosphatase complex allowing Pah1p to synthesize DAG which facilitates the formation of a lipid droplet at multiple regions of the ER. Droplets may not originate in areas that lack Nem1p/ Spo7p due to the inhibitory action of the DAG kinase (Dgk1p). In the absence of Dgk1p droplet formation is unregulated resulting in increased lipid droplet number.

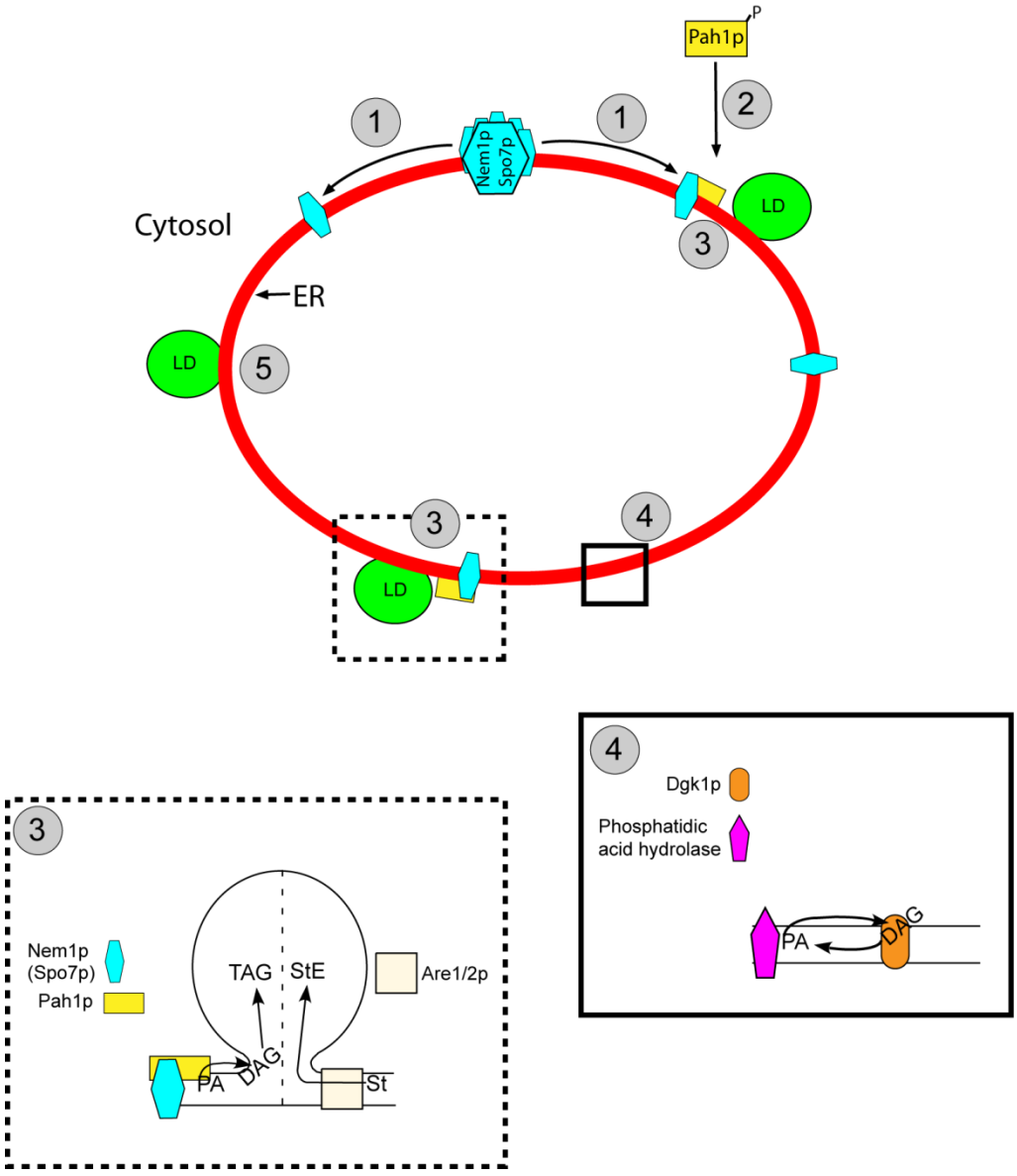

Figure 12. Hypothetical model showing the steps in Pah1p facilitated lipid droplet assembly. (1) Neutral lipid synthesis induces dispersion of the Nem1p/ Spo7p complex along the ER. (2) Pah1p associates with the ER membrane after dephosphorylation by Nem1p. (3) Association of Pah1p with the ER allows for the conversion of membrane PA to DAG to facilitate droplet formation or for TAG synthesis. (4) Droplets do not form in other regions of the ER due to the presence of inhibitory Dgk1p. (5) Droplets may also assemble via other pathways independent of Pah1p.

The role of diacylglycerol and other lipids on droplet formation

How diacylglycerol promotes droplet assembly still remains an unanswered question in this dissertation. The experiments reported here also cannot rule out the role of other phospholipids in the biogenesis of a droplet. The difficulty in understanding the role of specific lipids in droplet formation can be solved with a microsome-based cell-free system that allows for lipid droplet assembly (Marchesan et al., 2003). To these microsomes, lipids (such as DAG, PA and PC) can be added and their effect on lipid droplet formation (monitored by Erg6p levels in LD fractions after gradient ultracentrifugation) can be determined. The assay may also need to be performed with microsomes isolated from mutant cells such as:

(1) *dga1Δ lro1Δ* mutants to eliminate the chance of increased droplet formation (with DAG as an activator) being due to increased TAG synthesis by the TAG acyltransferases.

(2) *pah1Δ* mutants to determine if the addition of DAG alone (or other lipids) as an activator, would rescue the lipid droplet deficiency phenotype.

(3) *pah1Δ are1Δ are2Δ* mutants to determine if the addition of lipids can somehow stimulate droplet assembly.

Steryl ester synthesis and droplet formation

When *PAH1* is knocked out in the background of a strain that cannot synthesize StE, lipid droplets fail to assemble under normal laboratory growth conditions. One of the possible causes for this defect may be the presence of excessive unesterified sterols at the ER (stiffening the membrane) along with the absence of Pah1p synthesized DAG (to assist in droplet assembly). Fluorescence microscopy of filipin labeled mutant cells would confirm the accumulation of unesterified sterols within the ER membrane.

It would also be interesting to determine what environmental factor (hypoxia or temperature change) allows lipid droplets to assemble in the *pah1Δ are1Δ are2Δ* mutant and whether similar factors would facilitate droplet formation in *are1Δ are2Δ* mutants alone. These experiments can be performed by simply growing the mutant cell lines under the required conditions (hypoxic conditions or at 25 ºC) and visualizing droplet number by fluorescence microscopy (compared to cells cultured under normal laboratory conditions).

Lipin phosphatase in mammals

I demonstrated here that Nem1p localizes as a single punctum per cell, on the ER membrane, and in close proximity to lipid droplets. When TAG synthesis is induced (in the quad mutant that is unable to synthesize neutral lipids), Nem1p has a diffuse localization from which a majority of nascent lipid droplets

originate. Unlike Nem1p, its mammalian orthologue, Dullard, localizes in a punctuate pattern around the nuclear ER membrane, and inside the nucleus (Kim et al., 2007). However, it remains unknown whether this localization correlates with areas in the cell where lipid droplets are present. It is also unclear why Dullard would localize inside the nucleus, because the protein has a predicted membrane spanning sequence and would only be able to reside within the nucleus if soluble domains are separated from that transmembrane sequence (Siniossoglou et al., 1998). Nevertheless, similar to Dullard, diffuse Nem1p may also reside inside the nucleus and may function to retain dephosphorylated lipin within the nucleus to regulate the transcription of genes involved in phospholipid biosynthesis. Regulation of phospholipid biosynthesis might be required to maintain or modify the phospholipid content at the lipid droplet monolayer. However, for Nem1p or Dullard to retain lipin within the nucleus, it will have to interact with Spo7 or its mammalian orthologue within the nucleus as well. Such an association has not yet been observed.

Fld1p and lipid droplet biogenesis

It is clear from the time course studies on lipid droplet biogenesis that Fld1 relocates from the cortical to perinuclear regions of the ER in response droplet assembly. However, how Fld1p is targeted to lipid droplets or relocated to a different region of the ER still remains unanswered. The Goodman lab recently

discovered that Fld1p isolated from wild-type cells forms homoligomers of about nine subunits, while the orthologous mutant to the human seipin-A212P (Fld1p-G225P) formed much smaller oligomers (Binns et al., 2010). If the oligomerization state of Fld1p is triggered by droplet availability, it would be necessary to compare the oligomeric state of the Fld1p in both wild-type and the quad mutants.

The main observation from experiments to understand the function of Fld1p was that the protein was always associated with lipid droplets regardless of the amount of droplets present or neutral lipid content within it. Fld1p is still expressed and localized as patches on the ER when droplets are nonexistent, however, orphan patches were not as bright as Fld1p patches associated with lipid droplets (Figure 19 B). If Fld1p is important for droplet biogenesis, it may function to restrict large quantities of synthesized neutral lipids in the ER bilayer to regions where Fld1 resides prior to the maturation of a droplet (Figure 24). Fld1p may form fewer oligomers when droplets are absent, but oligomerization may be induced during neutral lipid synthesis to assist the formation of the droplet bud. Although it is yet to be confirmed that quad mutants have fewer Fld1p oligomers, the model does explain why orphan Fld1p patches (those observed in the quad mutant) are not as intense as Fld1p patches that interact with lipid droplets.

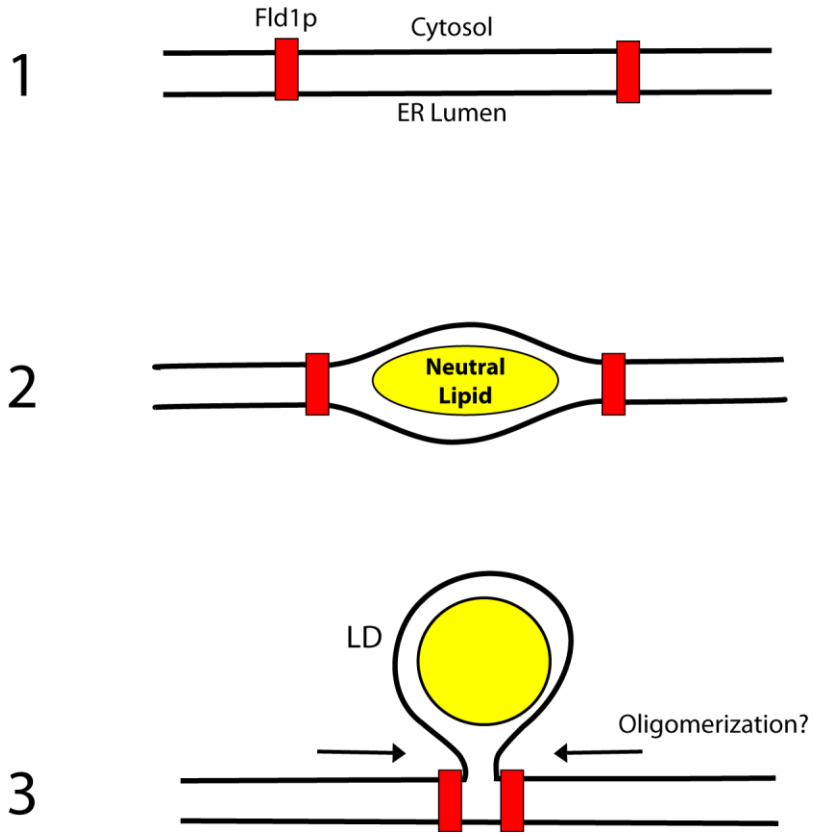

Figure 13. A model for how oligomerization of Fld1p may facilitate lipid droplet assembly. (1) The ER membrane without lipid droplets or neutral lipid synthesis. Fld1p molecules are far apart from each other resulting in low Fld1p-tdTomato fluorescence in quad mutants (Figure 19 B). (2) Fld1p restricts synthesized neutral lipids within the ER bilayer. (3) Oligomerization of Fld1p facilitates organized budding of lipid droplets. Brighter Fld1p-tdTomato signal observed in wild-type cells may be due to oligomerization.

Regardless of whether oligomeric state of Fld1 is altered in the presence or absence of lipid droplets, it is possible that posttranslational modifications to the protein triggers oligomerization or interaction with lipid droplets. Therefore, protein mass spectrometric analysis of Fld1p isolated from WT and quad mutants may be able to detect protein modifications between the two isolates. Nevertheless, we may understand more about seipin function if changes to isolated LD morphology are observed when purified Fld1p is added. Such an assay would also provide the opportunity to determine the regions of Fld1p responsible for any observed changes.

Lipid droplet assembly

It is understood that lipid droplets originate from the ER, however, no one has ever observed this event in detail. With a system to induce droplet formation already set up, it is possible to obtain transmission EM images highlighting the different steps in the assembly of a lipid droplet from multiple time points during the induction process. Even more valuable will be to compare the information obtained to similar experiments on cells that lack *FLD1*, because it would clarify whether the defects to droplet morphology in the mutant occur during or after the assembly of the droplet.

REFERENCES

Adeyo, O., P.J. Horn, S. Lee, D.D. Binns, A. Chandrahas, K.D. Chapman, and J.M. Goodman. 2011. The yeast lipin orthologue Pah1p is important for biogenesis of lipid droplets. *J Cell Biol*. 192:1043-1055.

Agarwal, A.K., and A. Garg. 2004. Seipin: a mysterious protein. *Trends Mol Med.* 10:440-444.

Agarwal, A.K., and A. Garg. 2006. Genetic basis of lipodystrophies and management of metabolic complications. *Annu Rev Med*. 57:297-311.

Antonny, B., I. Huber, S. Paris, M. Chabre, and D. Cassel. 1997. Activation of ADP-ribosylation factor 1 GTPase-activating protein by phosphatidylcholine-derived diacylglycerols. *The Journal of biological chemistry*. 272:30848-30851.

Asp, L., F. Kartberg, J. Fernandez-Rodriguez, M. Smedh, M. Elsner, F. Laporte, M. Barcena, K.A. Jansen, J.A. Valentijn, A.J. Koster, J.J. Bergeron, and T. Nilsson. 2009. Early stages of Golgi vesicle and tubule formation require diacylglycerol. *Mol Biol Cell*. 20:780-790.

Baba, M., M. Osumi, and Y. Ohsumi. 1995. Analysis of the membrane structures involved in autophagy in yeast by freeze-replica method. *Cell Struct Funct*. 20:465-471.

Bacia, K., P. Schwille, and T. Kurzchalia. 2005. Sterol structure determines the separation of phases and the curvature of the liquid-ordered phase in model membranes. *Proc Natl Acad Sci U S A.* 102:3272-3277.

Bartz, R., J.K. Zehmer, M. Zhu, Y. Chen, G. Serrero, Y. Zhao, and P. Liu. 2007. Dynamic activity of lipid droplets: protein phosphorylation and GTP-mediated protein translocation. *J Proteome Res*. 6:3256-3265.

Beller, M., D. Riedel, L. Jansch, G. Dieterich, J. Wehland, H. Jackle, and R.P. Kuhnlein. 2006. Characterization of the Drosophila lipid droplet subproteome. *Mol Cell Proteomics*. 5:1082-1094.

Binns, D., T. Januszewski, Y. Chen, J. Hill, V.S. Markin, Y. Zhao, C. Gilpin, K.D. Chapman, R.G. Anderson, and J.M. Goodman. 2006. An intimate collaboration between peroxisomes and lipid bodies. *J Cell Biol*. 173:719-731.

Binns, D., S. Lee, C.L. Hilton, Q.X. Jiang, and J.M. Goodman. 2010. Seipin is a discrete homooligomer. *Biochemistry*. 49:10747-10755.

Bligh, E.G., and W.J. Dyer. 1959. A rapid method of total lipid extraction and purification. *Can J Biochem Physiol*. 37:911-917.

Bozza, P.T., W. Yu, J.F. Penrose, E.S. Morgan, A.M. Dvorak, and P.F. Weller. 1997. Eosinophil lipid bodies: specific, inducible intracellular sites for enhanced eicosanoid formation. *J Exp Med*. 186:909-920.

Brasaemle, D.L., G. Dolios, L. Shapiro, and R. Wang. 2004. Proteomic analysis of proteins associated with lipid droplets of basal and lipolytically stimulated 3T3-L1 adipocytes. *The Journal of biological chemistry*. 279:46835-46842.

Brindley, D.N. 1984. Intracellular translocation of phosphatidate phosphohydrolase and its possible role in the control of glycerolipid synthesis. *Prog Lipid Res*. 23:115-133.

Brodsky, J.L., S. Hamamoto, D. Feldheim, and R. Schekman. 1993. Reconstitution of protein translocation from solubilized yeast membranes reveals topologically distinct roles for BiP and cytosolic Hsc70. *J Cell Biol*. 120:95-102.

Capuano, F., F. Beaudoin, J.A. Napier, and P.R. Shewry. 2007. Properties and exploitation of oleosins. *Biotechnol Adv*. 25:203-206.

Carman, G.M., and S.A. Henry. 2007. Phosphatidic acid plays a central role in the transcriptional regulation of glycerophospholipid synthesis in Saccharomyces cerevisiae. *The Journal of biological chemistry*. 282:37293-37297.

Carrasco, S., and I. Merida. 2007. Diacylglycerol, when simplicity becomes complex. *Trends Biochem Sci*. 32:27-36.

Chang, B.H., L. Li, A. Paul, S. Taniguchi, V. Nannegari, W.C. Heird, and L. Chan. 2006. Protection against fatty liver but normal adipogenesis in mice lacking adipose differentiation-related protein. *Mol Cell Biol*. 26:1063-1076.

Chen, W., V.K. Yechoor, B.H. Chang, M.V. Li, K.L. March, and L. Chan. 2009. The human lipodystrophy gene product Berardinelli-Seip congenital lipodystrophy 2/seipin plays a key role in adipocyte differentiation. *Endocrinology*. 150:4552-4561.

Cheng, J., A. Fujita, Y. Ohsaki, M. Suzuki, Y. Shinohara, and T. Fujimoto. 2009. Quantitative electron microscopy shows uniform incorporation of triglycerides into existing lipid droplets. *Histochem Cell Biol*. 132:281-291.

Choi, H.S., W.M. Su, J.M. Morgan, G.S. Han, Z. Xu, E. Karanasios, S. Siniossoglou, and G.M. Carman. 2011. Phosphorylation of phosphatidate phosphatase regulates its membrane association and physiological functions in Saccharomyces cerevisiae:

identification of SER(602), THR(723), AND SER(744) as the sites phosphorylated by CDC28 (CDK1)-encoded cyclin-dependent kinase. *The Journal of biological chemistry*. 286:1486-1498.

Czabany, T., A. Wagner, D. Zweytick, K. Lohner, E. Leitner, E. Ingolic, and G. Daum. 2008. Structural and biochemical properties of lipid particles from the yeast Saccharomyces cerevisiae. *The Journal of biological chemistry*. 283:17065-17074.

Dephoure, N., R.W. Howson, J.D. Blethrow, K.M. Shokat, and E.K. O'Shea. 2005. Combining chemical genetics and proteomics to identify protein kinase substrates. *Proc Natl Acad Sci U S A*. 102:17940-17945.

Donkor, J., M. Sariahmetoglu, J. Dewald, D.N. Brindley, and K. Reue. 2007. Three mammalian lipins act as phosphatidate phosphatases with distinct tissue expression patterns. *The Journal of biological chemistry*. 282:3450-3457.

Dvorak, A.M., E. Morgan, R.P. Schleimer, S.W. Ryeom, L.M. Lichtenstein, and P.F. Weller. 1992. Ultrastructural immunogold localization of prostaglandin endoperoxide synthase (cyclooxygenase) to non-membrane-bound cytoplasmic lipid bodies in human lung mast cells, alveolar macrophages, type II pneumocytes, and neutrophils. *J Histochem Cytochem*. 40:759-769.

Eastman, S.W., M. Yassaee, and P.D. Bieniasz. 2009. A role for ubiquitin ligases and Spartin/SPG20 in lipid droplet turnover. *J Cell Biol*. 184:881-894.

Fakas, S., C. Konstantinou, and G.M. Carman. 2011. DGK1-encoded diacylglycerol kinase activity is required for phospholipid synthesis during growth resumption from stationary phase in Saccharomyces cerevisiae. *The Journal of biological chemistry*. 286:1464-1474.

Faust, I.M., P.R. Johnson, J.S. Stern, and J. Hirsch. 1978. Diet-induced adipocyte number increase in adult rats: a new model of obesity. *Am J Physiol*. 235:E279-286.

Fei, W., G. Shui, B. Gaeta, X. Du, L. Kuerschner, P. Li, A.J. Brown, M.R. Wenk, R.G. Parton, and H. Yang. 2008. Fld1p, a functional homologue of human seipin, regulates the size of lipid droplets in yeast. *J Cell Biol*. 180:473-482.

Fei, W., G. Shui, Y. Zhang, N. Krahmer, C. Ferguson, T.S. Kapterian, R.C. Lin, I.W. Dawes, A.J. Brown, P. Li, X. Huang, R.G. Parton, M.R. Wenk, T.C. Walther, and H. Yang. 2011. A role for phosphatidic Acid in the formation of "supersized" lipid droplets. *PLoS Genet*. 7:e1002201.

Fei, W., H. Wang, X. Fu, C. Bielby, and H. Yang. 2009. Conditions of endoplasmic reticulum stress stimulate lipid droplet formation in Saccharomyces cerevisiae. *Biochem J*. 424:61-67.

Finck, B.N., M.C. Gropler, Z. Chen, T.C. Leone, M.A. Croce, T.E. Harris, J.C. Lawrence, Jr., and D.P. Kelly. 2006. Lipin 1 is an inducible amplifier of the hepatic PGC-1alpha/PPARalpha regulatory pathway. *Cell Metab*. 4:199-210.

Fischer, J., C. Lefevre, E. Morava, J.M. Mussini, P. Laforet, A. Negre-Salvayre, M. Lathrop, and R. Salvayre. 2007. The gene encoding adipose triglyceride lipase (PNPLA2) is mutated in neutral lipid storage disease with myopathy. *Nat Genet*. 39:28-30.

Fujimoto, T., and R.G. Parton. 2011. Not just fat: the structure and function of the lipid droplet. *Cold Spring Harb Perspect Biol*. 3.

Garbarino, J., M. Padamsee, L. Wilcox, P.M. Oelkers, D. D'Ambrosio, K.V. Ruggles, N. Ramsey, O. Jabado, A. Turkish, and S.L. Sturley. 2009. Sterol and diacylglycerol acyltransferase deficiency triggers fatty acid-mediated cell death. *The Journal of biological chemistry*. 284:30994-31005.

Gaspar, M.L., H.F. Hofbauer, S.D. Kohlwein, and S.A. Henry. 2011. Coordination of storage lipid synthesis and membrane biogenesis: evidence for cross-talk between triacylglycerol metabolism and phosphatidylinositol synthesis. *The Journal of biological chemistry*. 286:1696-1708.

Gaspar, M.L., S.A. Jesch, R. Viswanatha, A.L. Antosh, W.J. Brown, S.D. Kohlwein, and S.A. Henry. 2008. A block in endoplasmic reticulum-to-Golgi trafficking inhibits phospholipid synthesis and induces neutral lipid accumulation. *The Journal of biological chemistry*. 283:25735-25751.

Goñi, F.M., and A. Alonso. 1999. Structure and functional properties of diacylglycerols in membranes. *Progress Lipid Res*. 38:1-48.

Goodman, J.M. 2009. Demonstrated and inferred metabolism associated with cytosolic lipid droplets. *J Lipid Res*. 50:2148-2156.

Gordon, G.B., M.A. Barcza, and M.E. Bush. 1977. Lipid accumulation of hypoxic tissue culture cells. *Am J Pathol*. 88:663-678.

Guo, Y., T.C. Walther, M. Rao, N. Stuurman, G. Goshima, K. Terayama, J.S. Wong, R.D. Vale, P. Walter, and R.V. Farese. 2008. Functional genomic screen reveals genes involved in lipid-droplet formation and utilization. *Nature*. 453:657-661.

Hamilton, J.A. 1989. Interactions of triglycerides with phospholipids: incorporation into the bilayer structure and formation of emulsions. *Biochemistry*. 28:2514-2520.

Han, G.S., C.N. Johnston, and G.M. Carman. 2004. Vacuole membrane topography of the DPP1-encoded diacylglycerol pyrophosphate phosphatase catalytic site from Saccharomyces cerevisiae. *The Journal of biological chemistry*. 279:5338-5345.

Han, G.S., C.N. Johnston, X. Chen, K. Athenstaedt, G. Daum, and G.M. Carman. 2001. Regulation of the Saccharomyces cerevisiae DPP1-encoded diacylglycerol pyrophosphate phosphatase by zinc. *The Journal of biological chemistry*. 276:10126-10133.

Han, G.S., L. O'Hara, G.M. Carman, and S. Siniossoglou. 2008a. An unconventional diacylglycerol kinase that regulates phospholipid synthesis and nuclear membrane growth. *The Journal of biological chemistry*. 283:20433-20442.

Han, G.S., L. O'Hara, S. Siniossoglou, and G.M. Carman. 2008b. Characterization of the yeast DGK1-encoded CTP-dependent diacylglycerol kinase. *The Journal of biological chemistry*. 283:20443-20453.

Han, G.S., S. Siniossoglou, and G.M. Carman. 2007. The cellular functions of the yeast lipin homolog PAH1p are dependent on its phosphatidate phosphatase activity. *The Journal of biological chemistry*. 282:37026-37035.

Han, G.S., W.I. Wu, and G.M. Carman. 2006. The Saccharomyces cerevisiae Lipin homolog is a Mg2+-dependent phosphatidate phosphatase enzyme. *The Journal of biological chemistry*. 281:9210-9218.

Harris, T.E., T.A. Huffman, A. Chi, J. Shabanowitz, D.F. Hunt, A. Kumar, and J.C. Lawrence, Jr. 2007. Insulin controls subcellular localization and multisite phosphorylation of the phosphatidic acid phosphatase, lipin 1. *The Journal of biological chemistry*. 282:277-286.

Herker, E., C. Harris, C. Hernandez, A. Carpentier, K. Kaehlcke, A.R. Rosenberg, R.V. Farese, Jr., and M. Ott. 2010. Efficient hepatitis C virus particle formation requires diacylglycerol acyltransferase-1. *Nat Med*. 16:1295-1298.

Hevonoja, T., M.O. Pentikainen, M.T. Hyvonen, P.T. Kovanen, and M. Ala-Korpela. 2000. Structure of low density lipoprotein (LDL) particles: basis for understanding molecular changes in modified LDL. *Biochim Biophys Acta*. 1488:189-210.

Hubscher, G., D.N. Brindley, M.E. Smith, and B. Sedgwick. 1967. Stimulation of biosynthesis of glyceride. *Nature*. 216:449-453.

Huh, W.K., J.V. Falvo, L.C. Gerke, A.S. Carroll, R.W. Howson, J.S. Weissman, and E.K. O'Shea. 2003. Global analysis of protein localization in budding yeast. *Nature*. 425:686-691.

Ito, H., Y. Fukuda, K. Murata, and A. Kimura. 1983. Transformation of intact yeast cells treated with alkali cations. *J Bacteriol*. 153:163-168.

Kadereit, B., P. Kumar, W.J. Wang, D. Miranda, E.L. Snapp, N. Severina, I. Torregroza, T. Evans, and D.L. Silver. 2008. Evolutionarily conserved gene family important for fat storage. *Proc Natl Acad Sci U S A*. 105:94-99.

Karanasios, E., G.S. Han, Z. Xu, G.M. Carman, and S. Siniossoglou. 2010. A phosphorylation-regulated amphipathic helix controls the membrane translocation and function of the yeast phosphatidate phosphatase. *Proc Natl Acad Sci U S A*. 107:17539-17544.

Kim, C.A., M. Delepine, E. Boutet, H. El Mourabit, S. Le Lay, M. Meier, M. Nemani, E. Bridel, C.C. Leite, D.R. Bertola, R.K. Semple, S. O'Rahilly, I. Dugail, J. Capeau, M. Lathrop, and J. Magre. 2008. Association of a homozygous nonsense caveolin-1 mutation with Berardinelli-Seip congenital lipodystrophy. *J Clin Endocrinol Metab*. 93:1129-1134.

Kim, Y., M.S. Gentry, T.E. Harris, S.E. Wiley, J.C. Lawrence, Jr., and J.E. Dixon. 2007. A conserved phosphatase cascade that regulates nuclear membrane biogenesis. *Proc Natl Acad Sci U S A*. 104:6596-6601.

Klingenspor, M., P. Xu, R.D. Cohen, C. Welch, and K. Reue. 1999. Altered gene expression pattern in the fatty liver dystrophy mouse reveals impaired insulin-mediated cytoskeleton dynamics. *The Journal of biological chemistry*. 274:23078-23084.

Kobor, M.S., J. Archambault, W. Lester, F.C. Holstege, O. Gileadi, D.B. Jansma, E.G. Jennings, F. Kouyoumdjian, A.R. Davidson, R.A. Young, and J. Greenblatt. 1999. An unusual eukaryotic protein phosphatase required for transcription by RNA polymerase II and CTD dephosphorylation in S. cerevisiae. *Mol Cell*. 4:55-62.

Koh, Y.K., M.Y. Lee, J.W. Kim, M. Kim, J.S. Moon, Y.J. Lee, Y.H. Ahn, and K.S. Kim. 2008. Lipin1 is a key factor for the maturation and maintenance of adipocytes in the regulatory network with CCAAT/enhancer-binding protein alpha and peroxisome proliferator-activated receptor gamma 2. *The Journal of biological chemistry*. 283:34896-34906.

Kron, S.J. 2002. Digital time-lapse microscopy of yeast cell growth. *Methods Enzymol*. 351:3-15.

Kumar, Y., J. Cocchiaro, and R.H. Valdivia. 2006. The obligate intracellular pathogen Chlamydia trachomatis targets host lipid droplets. *Curr Biol*. 16:1646-1651.

Kurat, C.F., H. Wolinski, J. Petschnigg, S. Kaluarachchi, B. Andrews, K. Natter, and S.D. Kohlwein. 2009. Cdk1/Cdc28-dependent activation of the major triacylglycerol lipase Tgl4 in yeast links lipolysis to cell-cycle progression. *Mol Cell*. 33:53-63.

Laemmli, U.K. 1970. Cleavage of structural proteins during the assembly of the head of bacteriophage T4. *Nature*. 227:680-685.

Laffargue, A., A. de Kochko, and S. Dussert. 2007. Development of solid-phase extraction and methylation procedures to analyse free fatty acids in lipid-rich seeds. *Plant Physiol Biochem*. 45:250-257.

Langner, C.A., E.H. Birkenmeier, O. Ben-Zeev, M.C. Schotz, H.O. Sweet, M.T. Davisson, and J.I. Gordon. 1989. The fatty liver dystrophy (fld) mutation. A new mutant mouse with a developmental abnormality in triglyceride metabolism and associated tissue-specific defects in lipoprotein lipase and hepatic lipase activities. *The Journal of biological chemistry*. 264:7994-8003.

Leber, R., E. Zinser, G. Zellnig, F. Paltauf, and G. Daum. 1994. Characterization of lipid particles of the yeast, Saccharomyces cerevisiae. *Yeast*. 10:1421-1428.

Listenberger, L.L., A.G. Ostermeyer-Fay, E.B. Goldberg, W.J. Brown, and D.A. Brown. 2007. Adipocyte differentiation-related protein reduces the lipid droplet association of adipose triglyceride lipase and slows triacylglycerol turnover. *J Lipid Res*. 48:2751-2761.

Liu, P., Y. Ying, Y. Zhao, D.I. Mundy, M. Zhu, and R.G. Anderson. 2004. Chinese hamster ovary K2 cell lipid droplets appear to be metabolic organelles involved in membrane traffic. *The Journal of biological chemistry*. 279:3787-3792.

Loewen, C.J., M.L. Gaspar, S.A. Jesch, C. Delon, N.T. Ktistakis, S.A. Henry, and T.P. Levine. 2004. Phospholipid metabolism regulated by a transcription factor sensing phosphatidic acid. *Science*. 304:1644-1647.

Magre, J., M. Delepine, E. Khallouf, T. Gedde-Dahl, Jr., L. Van Maldergem, E. Sobel, J. Papp, M. Meier, A. Megarbane, A. Bachy, A. Verloes, F.H. d'Abronzo, E. Seemanova, R. Assan, N. Baudic, C. Bourut, P. Czernichow, F. Huet, F. Grigorescu, M. de Kerdanet, D. Lacombe, P. Labrune, M. Lanza, H. Loret, F. Matsuda, J. Navarro, A. Nivelon-Chevalier, M. Polak, J.J. Robert, P. Tric, N. Tubiana-Rufi, C. Vigouroux, J. Weissenbach, S. Savasta, J.A. Maassen, O. Trygstad, P. Bogalho, P. Freitas, J.L. Medina, F. Bonnicci, B.I. Joffe, G. Loyson, V.R. Panz, F.J. Raal, S. O'Rahilly, T. Stephenson, C.R. Kahn, M. Lathrop, and J.

Capeau. 2001. Identification of the gene altered in Berardinelli-Seip congenital lipodystrophy on chromosome 11q13. *Nat Genet*. 28:365-370.

Mah, A.S., A.E. Elia, G. Devgan, J. Ptacek, M. Schutkowski, M. Snyder, M.B. Yaffe, and R.J. Deshaies. 2005. Substrate specificity analysis of protein kinase complex Dbf2-Mob1 by peptide library and proteome array screening. *BMC Biochem*. 6:22.

Marchesan, D., M. Rutberg, L. Andersson, L. Asp, T. Larsson, J. Boren, B.R. Johansson, and S.O. Olofsson. 2003. A phospholipase D-dependent process forms lipid droplets containing caveolin, adipocyte differentiation-related protein, and vimentin in a cell-free system. *The Journal of biological chemistry*. 278:27293-27300.

McLauchlan, J. 2009. Hepatitis C virus: viral proteins on the move. *Biochem Soc Trans*. 37:986-990.

Miyanari, Y., K. Atsuzawa, N. Usuda, K. Watashi, T. Hishiki, M. Zayas, R. Bartenschlager, T. Wakita, M. Hijikata, and K. Shimotohno. 2007. The lipid droplet is an important organelle for hepatitis C virus production. *Nat Cell Biol*. 9:1089-1097.

Miyoshi, H., J.W. Perfield, 2nd, S.C. Souza, W.J. Shen, H.H. Zhang, Z.S. Stancheva, F.B. Kraemer, M.S. Obin, and A.S. Greenberg. 2007. Control of adipose triglyceride lipase action by serine 517 of perilipin A globally regulates protein kinase A-stimulated lipolysis in adipocytes. *The Journal of biological chemistry*. 282:996-1002.

Miyoshi, H., S.C. Souza, M. Endo, T. Sawada, J.W. Perfield, 2nd, C. Shimizu, Z. Stancheva, S. Nagai, K.J. Strissel, N. Yoshioka, M.S. Obin, T. Koike, and A.S. Greenberg. 2010. Perilipin overexpression in mice protects against diet-induced obesity. *J Lipid Res*. 51:975-982.

Murphy, D.J. 2001. The biogenesis and functions of lipid bodies in animals, plants and microorganisms. *Prog Lipid Res*. 40:325-438.

Nakamura, N., Y. Banno, and K. Tamiya-Koizumi. 2005. Arf1-dependent PLD1 is localized to oleic acid-induced lipid droplets in NIH3T3 cells. *Biochem Biophys Res Commun*. 335:117-123.

O'Hara, L., G.S. Han, S. Peak-Chew, N. Grimsey, G.M. Carman, and S. Siniossoglou. 2006. Control of phospholipid synthesis by phosphorylation of the yeast lipin Pah1p/Smp2p Mg2+-dependent phosphatidate phosphatase. *The Journal of biological chemistry*. 281:34537-34548.

Oelkers, P., D. Cromley, M. Padamsee, J.T. Billheimer, and S.L. Sturley. 2002. The DGA1 gene determines a second triglyceride synthetic pathway in yeast. *The Journal of biological chemistry*. 277:8877-8881.

Pagano, R.E., and K.J. Longmuir. 1985. Phosphorylation, transbilayer movement, and facilitated intracellular transport of diacylglycerol are involved in the uptake of a fluorescent analog of phosphatidic acid by cultured fibroblasts. *The Journal of biological chemistry*. 260:1909-1916.

Patel, H., H. Cross, C. Proukakis, R. Hershberger, P. Bork, F.D. Ciccarelli, M.A. Patton, V.A. McKusick, and A.H. Crosby. 2002. SPG20 is mutated in Troyer syndrome, an hereditary spastic paraplegia. *Nat Genet*. 31:347-348.

Peterfy, M., T.E. Harris, N. Fujita, and K. Reue. 2010. Insulin-stimulated interaction with 14-3-3 promotes cytoplasmic localization of lipin-1 in adipocytes. *The Journal of biological chemistry*. 285:3857-3864.

Peterfy, M., J. Phan, P. Xu, and K. Reue. 2001. Lipodystrophy in the fld mouse results from mutation of a new gene encoding a nuclear protein, lipin. *Nat Genet*. 27:121-124.

Peterson, T.R., S.S. Sengupta, T.E. Harris, A.E. Carmack, S.A. Kang, E. Balderas, D.A. Guertin, K.L. Madden, A.E. Carpenter, B.N. Finck, and D.M. Sabatini. 2011. mTOR Complex 1 Regulates Lipin 1 Localization to Control the SREBP Pathway. *Cell*. 146:408-420.

Petschnigg, J., H. Wolinski, D. Kolb, G. Zellnig, C.F. Kurat, K. Natter, and S.D. Kohlwein. 2009. Good fat, essential cellular requirements for triacylglycerol synthesis to maintain membrane homeostasis in yeast. *The Journal of biological chemistry*. 284:30981-30993.

Ploegh, H.L. 2007. A lipid-based model for the creation of an escape hatch from the endoplasmic reticulum. *Nature*. 448:435-438.

Prattes, S., G. Horl, A. Hammer, A. Blaschitz, W.F. Graier, W. Sattler, R. Zechner, and E. Steyrer. 2000. Intracellular distribution and mobilization of unesterified cholesterol in adipocytes: triglyceride droplets are surrounded by cholesterol-rich ER-like surface layer structures. *J Cell Sci*. 113 (Pt 17):2977-2989.

Ptacek, J., G. Devgan, G. Michaud, H. Zhu, X. Zhu, J. Fasolo, H. Guo, G. Jona, A. Breitkreutz, R. Sopko, R.R. McCartney, M.C. Schmidt, N. Rachidi, S.J. Lee, A.S. Mah, L. Meng, M.J. Stark, D.F. Stern, C. De Virgilio, M. Tyers, B. Andrews, M. Gerstein, B. Schweitzer, P.F. Predki, and M. Snyder. 2005. Global analysis of protein phosphorylation in yeast. *Nature*. 438:679-684.

Qi, L., H. Shen, I. Larson, E.J. Schaefer, A.S. Greenberg, D.A. Tregouet, D. Corella, and J.M. Ordovas. 2004. Gender-specific association of a perilipin gene haplotype with obesity risk in a white population. *Obes Res*. 12:1758-1765.

Rehnmark, S., C.S. Giometti, B.G. Slavin, M.H. Doolittle, and K. Reue. 1998. The fatty liver dystrophy mutant mouse: microvesicular steatosis associated with altered expression levels of peroxisome proliferator-regulated proteins. *J Lipid Res*. 39:2209-2217.

Reue, K., P. Xu, X.P. Wang, and B.G. Slavin. 2000. Adipose tissue deficiency, glucose intolerance, and increased atherosclerosis result from mutation in the mouse fatty liver dystrophy (fld) gene. *J Lipid Res*. 41:1067-1076.

Robenek, H., O. Hofnagel, I. Buers, M.J. Robenek, D. Troyer, and N.J. Severs. 2006. Adipophilin-enriched domains in the ER membrane are sites of lipid droplet biogenesis. *J Cell Sci*. 119:4215-4224.

Robenek, H., M.J. Robenek, and D. Troyer. 2005. PAT family proteins pervade lipid droplet cores. *J Lipid Res*. 46:1331-1338.

Robenek, M.J., N.J. Severs, K. Schlattmann, G. Plenz, K.P. Zimmer, D. Troyer, and H. Robenek. 2004. Lipids partition caveolin-1 from ER membranes into lipid droplets: updating the model of lipid droplet biogenesis. *FASEB J*. 18:866-868.

Roth, M.G. 1999. Lipid regulators of membrane traffic through the Golgi complex. *Trends Cell Biol*. 9:174-179.

Samsa, M.M., J.A. Mondotte, N.G. Iglesias, I. Assuncao-Miranda, G. Barbosa-Lima, A.T. Da Poian, P.T. Bozza, and A.V. Gamarnik. 2009. Dengue virus capsid protein usurps lipid droplets for viral particle formation. *PLoS Pathog*. 5:e1000632.

Santos-Rosa, H., J. Leung, N. Grimsey, S. Peak-Chew, and S. Siniossoglou. 2005. The yeast lipin Smp2 couples phospholipid biosynthesis to nuclear membrane growth. *EMBO J*. 24:1931-1941.

Sato, S., M. Fukasawa, Y. Yamakawa, T. Natsume, T. Suzuki, I. Shoji, H. Aizaki, T. Miyamura, and M. Nishijima. 2006. Proteomic profiling of lipid droplet proteins in hepatoma cell lines expressing hepatitis C virus core protein. *J Biochem*. 139:921-930.

Schweiger, M., A. Lass, R. Zimmermann, T.O. Eichmann, and R. Zechner. 2009. Neutral lipid storage disease: genetic disorders caused by mutations in adipose triglyceride lipase/PNPLA2 or CGI-58/ABHD5. *Am J Physiol Endocrinol Metab*. 297:E289-296.

Sikorski, R.S., and P. Hieter. 1989. A system of shuttle vectors and yeast host strains designed for efficient manipulation of DNA in Saccharomyces cerevisiae. *Genetics*. 122:19-27.

Siniossoglou, S., H. Santos-Rosa, J. Rappsilber, M. Mann, and E. Hurt. 1998. A novel complex of membrane proteins required for formation of a spherical nucleus. *EMBO J*. 17:6449-6464.

Skinner, J.R., T.M. Shew, D.M. Schwartz, A. Tzekov, C.M. Lepus, N.A. Abumrad, and N.E. Wolins. 2009. Diacylglycerol enrichment of endoplasmic reticulum or lipid droplets recruits perilipin 3/TIP47 during lipid storage and mobilization. *The Journal of biological chemistry*. 284:30941-30948.

Syed, G.H., Y. Amako, and A. Siddiqui. 2010. Hepatitis C virus hijacks host lipid metabolism. *Trends Endocrinol Metab*. 21:33-40.

Szymanski, K.M., D. Binns, R. Bartz, N.V. Grishin, W.P. Li, A.K. Agarwal, A. Garg, R.G. Anderson, and J.M. Goodman. 2007. The lipodystrophy protein seipin is found at endoplasmic reticulum lipid droplet junctions and is important for droplet morphology. *Proc Natl Acad Sci U S A*. 104:20890-20895.

Tauchi-Sato, K., S. Ozeki, T. Houjou, R. Taguchi, and T. Fujimoto. 2002. The surface of lipid droplets is a phospholipid monolayer with a unique Fatty Acid composition. *The Journal of biological chemistry*. 277:44507-44512.

Umlauf, E., E. Csaszar, M. Moertelmaier, G.J. Schuetz, R.G. Parton, and R. Prohaska. 2004. Association of stomatin with lipid bodies. *The Journal of biological chemistry*. 279:23699-23709.

Valachovic, M., B.M. Bareither, M. Shah Alam Bhuiyan, J. Eckstein, R. Barbuch, D. Balderes, L. Wilcox, S.L. Sturley, R.C. Dickson, and M. Bard. 2006. Cumulative mutations affecting sterol biosynthesis in the yeast Saccharomyces cerevisiae result in synthetic lethality that is suppressed by alterations in sphingolipid profiles. *Genetics*. 173:1893-1908.

Waltermann, M., and A. Steinbuchel. 2005. Neutral lipid bodies in prokaryotes: recent insights into structure, formation, and relationship to eukaryotic lipid depots. *J Bacteriol*. 187:3607-3619.

Walther, T.C., and R.V. Farese, Jr. 2009. The life of lipid droplets. *Biochim Biophys Acta*. 1791:459-466.

Wan, H.C., R.C. Melo, Z. Jin, A.M. Dvorak, and P.F. Weller. 2007. Roles and origins of leukocyte lipid bodies: proteomic and ultrastructural studies. *FASEB J*. 21:167-178.

Wang, H., L. Hu, K. Dalen, H. Dorward, A. Marcinkiewicz, D. Russell, D. Gong, C. Londos, T. Yamaguchi, C. Holm, M.A. Rizzo, D. Brasaemle, and C. Sztalryd. 2009. Activation of hormone-sensitive lipase requires two steps, protein phosphorylation and binding to the PAT-1 domain of lipid droplet coat proteins. *The Journal of biological chemistry*. 284:32116-32125.

White, M.J., J.P. Hirsch, and S.A. Henry. 1991. The OPI1 gene of Saccharomyces cerevisiae, a negative regulator of phospholipid biosynthesis, encodes a protein containing polyglutamine tracts and a leucine zipper. *The Journal of biological chemistry*. 266:863-872.

Windpassinger, C., M. Auer-Grumbach, J. Irobi, H. Patel, E. Petek, G. Horl, R. Malli, J.A. Reed, I. Dierick, N. Verpoorten, T.T. Warner, C. Proukakis, P. Van den Bergh, C. Verellen, L. Van Maldergem, L. Merlini, P. De Jonghe, V. Timmerman, A.H. Crosby, and K. Wagner. 2004. Heterozygous missense mutations in BSCL2 are associated with distal hereditary motor neuropathy and Silver syndrome. *Nat Genet*. 36:271-276.

Wolinski, H., and S.D. Kohlwein. 2008. Microscopic analysis of lipid droplet metabolism and dynamics in yeast. *Methods in molecular biology (Clifton, N.J*. 457:151-163.

Wright, R. 2000. Transmission electron microscopy of yeast. *Microsc Res Tech*. 51:496-510.